Impact of continuous temperature variations on the strength of railway line steel

by

CHRINAH NOMBULELO KETWA

Thesis submitted in fulfilment of the requirements for the degree

Master of Engineering: Mechanical Engineering

in Mechanical and Mechatronic Engineering Department

in the Faculty of Engineering and the Built Environment

at the Cape Peninsula University of Technology

Supervisor: Dr V. Msomi

Bellville

Submission date: 15 March 2022

DECLARATION

I; Chrinah Nombulelo Ketwa, declare that the contents of this thesis represent my own unaided work, and that the thesis has not previously been submitted for academic examination towards any qualification. Furthermore, it represents my own opinions and not necessarily those of Cape Peninsula University of Technology or Transnet Freight Rail.

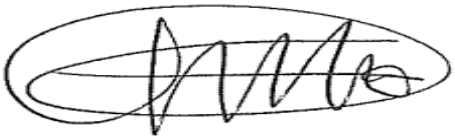

15 March 2022

Sign

Date

ABSTRACT

This research focuses on the impact of temperature variations on the mechanical properties of railway line steel. Railway line steel must be made from a strong material that endures wear, fatigue, and various temperature effects in order for the railway transport to supply an uninterrupted service of goods to customers. The mechanical properties of the structural materials strongly depend on their microstructure. The fatigue tests were conducted, and repeated linear load tests were applied to check the behaviour of the material. The reports released by the Railway Safety Regulator in South Africa 2017 reveal many defects found on the railway lines, and it cannot at this point be determined how they develop to the state of disturbing the transport service.

Many researchers agree that temperature can have an impact on the steel, but it is not yet clear how temperature can affect the material properties of railway line steel. This research has discovered that temperature has an effect on mechanical properties of the steel. The microstructure results have shown that fatigue load causes microstructure grain transformation, dislocating element grains. The results have shown that as the temperature increases due to repeated cycle loading, carbon content decreases, so the steel hardens increased to 443.3 HV0.5. It is assumed that crack defects develop on the areas where brittleness has become the highest.

Further research is needed to effectively evaluate and compare a sample which has been in use and a virgin sample to see the actual appearance of the microstructure results of both, this will help in defining the maximum lifetime of the rail steel and to know when it can be replaced.

Keywords: temperature, rail steel, microstructure, fatigue, wear

ACKNOWLEDGEMENT

I would like to express my special thanks and gratitude to my supervisor Doctor Msomi who gave me an exciting opportunity to do this wonderful research project which has extended my knowledge in Material Science. I thank the Lab Technicians for their assistance in preparing and testing my specimens.

My family members have been so great to me in the pursuit of this project. I would like to thank my mother and my grandmother; whose love and guidance are with me in whatever I pursue, they are my ultimate role models. Most importantly, I wish to thank my loving and supportive three wonderful children, Wendy, Siyamthanda and Ayolise, who have been providing an unending inspiration and finally I thank the Radana family for warmly opening their home for myself and my kids.

LIST OF FIGURES

Figure 1.1: Overcrowded railway vehicle in Cape Town area (Malan, 2014) 15
Figure 1.2: Geographical distribution of consequences due to derailments expressed as fatality and weighted injury (FWI) (State of Safety Report 2019/20) 16
Figure 1.3: Loaded freight rail from Bellville Transnet yard (Conradie, 2012) 16
Figure 3.1: Instron Machine 8801 - Fatigue Testing System 37
Figure 3.2 Struers LaboPress-3 Thermal Compression Moulding Machine 38
Figure 3.3: Struers LaboPress-3 Thermal Compression Moulding Machine 39
Figure 3.4: Inverted metallurgical microscope, AE2000 MET 40
Figure 3.5: LM Plan Achromatic inverted microscope objectives: nosepieces 40
Figure 3.6: InnovaTest Falcon 505 Machine – microhardness tester 41
Figure 3.7: Scanning Electron Microscope (SEM) analysis with energy dispersive X-ray from UCT 43
Figure 3.8: a) Side view of test piece for fatigue test; b) bottom view; c) top view; d) sample fitted on Instron machine for fatigue test 44
Figure 3.9: Test specimens a) targeted position on rail line head for fatigue test; b) cut-out of specimen; c) specimen dimensions; d) mounted specimen dimensions 45
Figure 3.10: Polishing chemicals a) F3µm diamond suspension and AKA-Lube/DP-blue; b) 0.2µm OP solution 47
Figure 3.11: Etched specimens ready for analysis 47
Figure 4.1: (a): Optical Microscope Micrograph – base material (a) at low resolution; (b) at high resolution 51
Figure 4.2: Optical Microscope Micrograph – Specimen 1 (a) at low resolution; (b) at high resolution 52
Figure 4.3: Optical Microscope Micrograph – Specimen 2 (a) at low resolution; (b) at high resolution 52
Figure 4.4: Optical Microscope Micrograph – Specimen 3 (a) at low resolution; (b) at high resolution 52
Figure 4.5: SEM micrographs of experimented rail steel showing elements transformation: (a) base metal; (b) Specimen 1; (c) Specimen 2 with element identification; (d) Specimen 3 showing clear cementite transformation 55
Figure 4.6: EDXS analysis (a) base material; (b) Specimen 1; (c) Specimen 2; (d) Specimen 3 58
Figure 4.7: EDXS patterns of rail steel (a) base material – no fatigue load applied; (b) Specimen 1 – loaded for 6 min; (c) Specimen 2 – loaded for 8 min; (d) Specimen 3 – loaded for 10 min 59
Figure 4.8: Specimens tested for microhardness showing test pattern (a) base material sample; (b) Specimen 1; (c) Specimen 2; (d) Specimen 3 60

Figure 4.9: Microhardness profiles (a) base material; (b) Specimen 1; (c) Specimen 2; (d) Specimen 3..... 63

LIST OF TABLES

Table 3.1: Specimen preparation method 46
Table 4.1: Chemical composition impurities of a base metal at room temperature 56
Table 4.2: Chemical composition impurities of Specimen 1 at room temperature 56
Table 4.3: Chemical composition impurities of Specimen 2 at room temperature 57
Table 4.4: Chemical composition impurities of Specimen 3 at room temperature 57
Table 4.5: Hardness statistical analysis: Vickers microhardness results (HV0.5) 64

LIST OF SYMBOLS

Unit	Description
C	Carbon
Al	Aluminium
Mn	Manganese
Fe	Iron
Si	Silicon
Cr	Chromium

TABLE OF CONTENTS

DECLARATION **1**

ABSTRACT **2**

ACKNOWLEDGEMENT **3**

LIST OF FIGURES **4**

LIST OF SYMBOLS **7**

1. CHAPTER 1 ..... **10**

INTRODUCTION 10
1.0 Introduction *10*
1.1 Rail track production process *10*
1.2 Factors affecting rail lives *12*
1.2.1 Corrosion 12
1.2.2 Wear 13
1.2.3 Rolling contact fatigue 13
1.2.4 Thermal expansion 13
1.3 Problem statement *14*
1.4 Background *14*
1.5 Aim and objectives *17*
1.6 Thesis organisation *17*

2. CHAPTER 2 ..... **19**

LITERATURE REVIEW 19
2.0 Introduction *19*
2.1 Factors influencing mechanical properties of rail steel *19*
2.2 Impact of temperature on mechanical properties of rail steel *21*
2.3 Rolling contact fatigue defects due to temperature variation *24*
2.4 Impact of temperature variation on rail steel performance *27*
2.5 Impact of change of weather conditions on rail steel behaviour *30*
2.6 Factors transforming microstructure of rail steel *32*
2.7 Summary *34*

3. CHAPTER 3 ..... **36**

EXPERIMENTAL SETUP AND PERFORMANCE 36
3.0 Introduction *36*
3.1 Experimental setup *36*
3.2 Description of equipment *36*
3.2.1 Instron Machine 8801 Servo-hydraulic Fatigue Testing System 37
3.2.2 Struers LaboPress-3 Thermal Compression Moulding Machine 38
3.2.3 Struers LaboPress-5 Polishing Machine 39
3.2.4 Inverted metallurgical microscope, AE2000 MET 40
3.2.5 InnovaTest Falcon 505 Vickers Microhardness Tester 41
3.2.6 Scanning Electron Microscope (SEM) analysis with energy dispersive X-ray 42
3.3 Preparation and performance of experiments *43*
3.3.1 Preparation of specimens for fatigue performance 43
3.3.2 Performance of fatigue test 44
3.3.3 Preparation of specimens for test analysis 45
3.4 Microstructure analysis *48*
3.5 Microstructure characterisation *48*
3.6 Microhardness analysis *49*

4 CHAPTER 4 50

EXPERIMENTAL RESULTS AND DISCUSSION 50
4.0 Introduction 50
4.1 Microstructure results 50
4.2 SEM microstructure analysis 53
4.2.1 Energy dispersive X-ray analysis 55
4.2.2 Energy dispersive X-ray spectrum analysis (EDXS) 58
4.3 Microhardness observation and analysis 60
4.3.1 Microhardness test pattern 60
4.3.2 Microhardness results 61

5. CHAPTER 5 65

CONCLUSION AND RECOMMENDATIONS 65
5.1 Conclusion 65
5.2 Recommendations 66

LIST OF REFERENCES 67

CHAPTER 1

INTRODUCTION

1.0 Introduction

Railway track is a structure that provides a levelled surface for the movement of railway vehicles. It consists mainly of rails, sleepers, fishplates and fasteners. The main component of the railway track is the rail, and it is made of a very strong material. The steel used to make rails must withstand stresses induced by the load applied (vertical, lateral, and longitudinal) to the rail during operation. Therefore, to withstand these stresses, the properties of rail-wheel material should possess high yield strength, toughness/tensile strength, hardness, wear and fatigue resistance (Bhadeshia *et al.,* 2011).

The steels that are normally used on railway rails are carbon-manganese steels with a pearlitic microstructure. Mechanical properties, achieved through the control of these compositions, ensure a safe railway system operation. Carbon and manganese content play a vital role in rail steel, such that the increase in carbon content in pearlitic steel improves strength properties, while alternatively, manganese content decreases the ability for the pearlitic transition (Ueda & Matsuda, 2019; Aniolek & Herian, 2008).

1.1 Rail track production process

To meet the requirements of high-quality steel with good microstructure and strong mechanical properties, a proper manufacturing process of rail steel is employed. The steel is processed in many steps to ensure the accuracy of the steel composition. These steps include pre-treatment, refining, vacuum degassing, continuous bloom casting, heat treatment, straightening, inspection, sawing, and drilling, all performed following

modern technology (Anyang General International Co [AGICO] Group, 2020).

- *Pre-treatment:* A process which reduces the content of harmful impurities in the molten steel. It dephosphatises and desulfurises the molten steel in the metal boiler in the blast furnace and then decarburises the molten steel in the converter.

- *Refining:* This process takes place outside the furnace; its main function is to further remove impurities and adjust steel elements and temperature of the molten steel.

- *Vacuum degassing:* This reduces the content of gases trapped in the molten steel such as hydrogen, oxygen and other gases, thereby improving the toughness of the steel.

- *Continuous bloom casting:* In this process, the steel is formed into a rectangular solid slab. The molten steel is carried by a ladle to the tundish which distributes it in small, uniform amounts to the moulds. The moulds extract heat from the molten steel as efficiently as possible; steel then solidifies on the outer side when it leaves the mould while the core is still molten but continues to cool to solidify. The small amount supplied allows for a faster cooling rate of the steel and uniform density to improve the macrostructure of the final steel product.

- *Rolling:* In this process, the slabs are formed into a rail shape either by groove or universal rolling machine. The steel slabs are directly pushed into the rolling mill which compresses the rectangular steel and forms an I-shape. This compression stretches the length almost to four times its original length.

- *Heat treatment:* This process stabilises the microstructure of the rail and drastically improves the mechanical property. The most popular heating technology is quenching, and tempering heat treatments are the most popular heat treatments. In addition, it undergoes a walking beam furnace heat treatment which controls the gas fractionation and prevents the decarburisation.

- *Straightening:* This is the final step in the manufacturing of a rail steel, done after cooling through rollers to increase the yield, reduce the residue stress and lengthen the service life of the rail steel.

- *Inspection, sawing and drilling:* These steps follow to complete the whole process.

1.2 Factors affecting rail lives

Rails do not last forever; their lives degrade. Corrosion, wear, rolling contact fatigue and thermal expansion are the main contributing factors that affect rail lives. Mitigating factors as to what can be done to overcome these common issues are discussed below.

1.2.1 Corrosion

Excessive corrosion is one of the main contributing factors that affects rail lives. Corrosion is mostly caused by weather conditions, constant exposure of the rails to moisture and sodium chloride in locations near the oceans. Corrosion has different effects on different parts of rail, but corrosion of the rail head can be a serious issue. Corrosion generally leads to the development of cracks in regions with a high concentration of stresses.

Corroded rail heads or a build-up of debris on them distracts electrical contact so contact can be lost entirely, and that can render the signalling

system unable to detect the train location; obviously this leads to performance and safety hazards. For the rails to survive this issue, one must manually weld a zig-zag bead of stainless steel across the rail head to ensure that electrical contact is not distracted, and therefore the signal does not break. For the endurance of rail under harsh conditions which accelerate the corrosion process, coating is the most suitable technology for protection. This coating provides high corrosion resistance and high abrasion resistance with long-term durability (Xu *et al.*, 2021).

1.2.2 Wear

Another main contributing factor that affects rail lives is wear. Rail wear is due to repeated wheel contact on rails which results in significant material loss from the rail. Lubrication is used to reduce the wear of the rail. However, side wear, which primarily occurs in curved rails and high traffic level areas, requires rail replacement depending on the severity of wear (Zhou *et al.*, 2020).

1.2.3 Rolling contact fatigue

Rolling contact fatigue (RCF) is another contributing factor that affects rail lives. Wheels rolling over the rail surface exert extremely high stress on the surface. This causes fatigue cracks at the surface of the rail once it reaches a certain extent of plastic deformation. There are many different types of RCF, namely gauge corner cracking, shelling and snakeskin. An S shaped cracking is a symbol representing RCF around the gauge corner of the rail (Chen *et al.*, 2019).

1.2.4 Thermal expansion

Thermal expansion also contributes to reducing rail lives. When temperatures change, objects change size, sometimes even imperceptibly. An increase of temperature causes expansion of objects, and a decrease of

temperature causes objects to contract. The rails are usually stretched into position during installation to deal with this thermal expansion and contraction. This helps during cold weather, as rails contract; therefore, they operate under greater tensile stress. The more tension applied, the smaller the force required to break the rail. Hence, rail failures are more likely in cold weather than in hot weather (Pyke, 2020).

1.3 Problem statement

Railway lines support and guide railway vehicles safely and efficiently. Railway lines are made of a material that is assumed to be strong enough to withstand wear, rolling contact fatigue damage or various temperature effects. The mechanical properties of railway lines are strongly dependent on the microstructural arrangement of the material used to manufacture them. It is well known that microstructural changes of any material can be affected by various factors. For rails, this includes load changes and thermal changes. There are numerous railway defects typically observed on railway lines of South Africa, but their origin is remains unknown. This suggests that various studies need to be conducted with the purpose of identifying the cause of specific problems that South African railway lines are facing. This current work aims to analyse the microstructural changes that occur when the railway line is subjected to uniform fatigue under different temperatures.

1.4 Background

Railway transport is one of the most popular modes of transport service in South Africa, predominantly owned by the state. Railway transport is acknowledged as the most used mode of transport for humans and goods worldwide since it is one of the cheapest modes of transport. The recent increase in reliance on this mode of transport suggests an increase in the number of trains to match the demand. This then leads to a rise in traffic volume which has an impact on the service life of railways. The life span of the railway line gets reduced due to repeated rolling contact which might

lead to rail surface damage. Figure 1.1 shows a dangerous method of passenger riding, indicating the need for more trains: here, the train is full inside, so commuters are hanging on the outside of the train. Commuters are overcrowding the first train to arrive, as they do not wait for the next incoming train because it might come late or not arrive at all due to technical problems.

Figure 1.1: Overcrowded railway vehicle in Cape Town area (Malan, 2014)

Figure 1.2 shows a geographical distribution of derailment concerns in the country. The graph indicates that big cities, which are the places with the highest demand of rail vehicles, are experiencing many derailments, potentially due to rail line defects which can be caused by frequent contact of wheel and rail during the travelling of a rail vehicle.

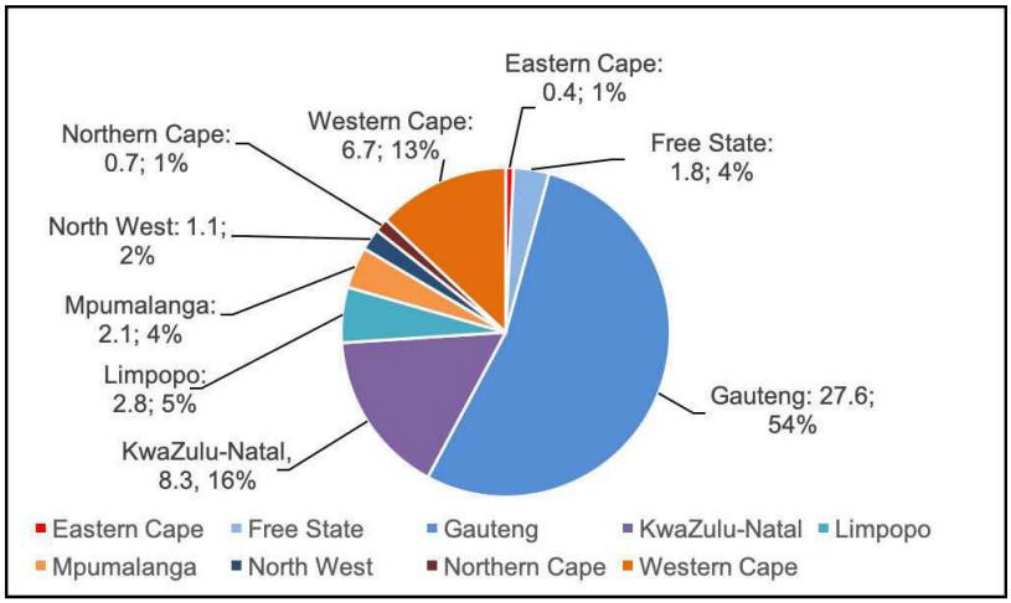

Figure 1.2: Geographical distribution of consequences due to derailments expressed as fatality and weighted injury (FWI) (State of Safety Report 2019/20)

Figure 1.3: Loaded freight rail from Bellville Transnet yard (Conradie, 2012)

Figure 1.3 shows a coal freight rail fully loaded, departing from Transnet yard in Bellville.

An increase in train speed, reliability and safety should be the focus areas for railway companies. Railway lines require several mechanical and functional properties such as wear resistance, deformation resistance and high fatigue life on railway steel.

This research aims to analyse the impact of temperature variation together with fatigue on the railway line steel, as this is assumed to be a factor contributing to the formation of defects.

1.5 Aim and objectives

The main aim of this study is to analyse the impact of varying temperature conditions coupled with fatigue on the mechanical properties of the railway line. This aim will be achieved through the following objectives:

- The specimens subjected to fatigue loading will be studied comparatively with the fresh specimens.
- Examine the impact of temperature variation caused by repeated cycle loading induced by the rail vehicle when it is in motion.
- Determine the relationship between fatigue load, time, and hardness to the microstructure of the rail steel.

1.6 Thesis organisation

There are five chapters presented in this thesis which provide information related to the method in which the research was conducted.

Chapter 1: **Introduction**: In this chapter, background is provided to give scope to the research; the research methodology is briefly explained; and the research delineation is identified. A high-level overview of the chapter and the content of the research is given. The chapter concludes with a list of primary research objectives.

Chapter 2: Literature Review: In this chapter, an in-depth literature review is conducted on the concept of impact of temperature variation on railway line steel microstructure.

Chapter 3: Experimental Setup and Performance: Data collection and research methodology are discussed in depth in this chapter. The experimenting process is defined and the approach to data collection is clarified. The chapter concludes with a list of results obtained during the experimental process.

Chapter 4: Experimental Results and Discussion: The results of experiments conducted in Chapter 3 are analysed and interpreted in detail in this chapter.

Chapter 5: Conclusion and Recommendations: The research is concluded, and recommendations are provided.

CHAPTER 2

LITERATURE REVIEW

2.0 Introduction

This chapter reports on the work surrounding the subject of failures occurring on railway lines due to temperature change. It starts with an in-depth discussion of temperature effects on mechanical properties of the rail steel, including its microstructure, and concludes by discussing defects developing on the rail steel due to temperature variation.

2.1 Factors influencing mechanical properties of rail steel

There are various factors that can affect the mechanical properties of the rail material such as hardness, strength, ductility, toughness, wear and corrosion resistance. The major factors include thermal variation and unintended chemical exposure of the rail. There are various ways that the rail material can be exposed in these factors. These include sudden change in weather conditions (thermal variations) and leakage of chemicals being transported via railway vehicles. Studies have been conducted to analyse the impact of various factors on the mechanical properties of rail materials.

Outinen and Makelainen (2004) have conducted extensive experimental research since 1994. For example, they have investigated mechanical properties of several structural steels at elevated temperatures to determine the temperature dependencies of the mechanical properties, using the transient state tensile test method. Their findings for structural steels S350GD+Z and S355J2H showed that mechanical properties such as yield strength, modulus of elasticity and thermal elongation of cold-formed steel after heating do not change much, as they remain at around the nominal values of the material. They reported that the behaviour of mechanical

properties at different temperatures should be well known to best understand the behaviour of steel and composite structures after heat.

According to Matsumura *et al.* (1991), the mechanical properties of a material are those properties that involve a reaction to an applied load. The mechanical properties of metals determine the range of usefulness of a material and establish the service life that can be expected; they also help to classify and identify material. Kang *et al.* (2021) claim in their recent study that there are two forces acting on the rail tracks: vertical and transverse force. Transverse force becomes larger on curved areas or on bridges where additional stresses are induced and superimposed in the rail foot. According to Kang *at al*., under cycle wheel load, the edge of the rail foot experiences larger stresses than the centre of the rail foot. These forces need to be taken into consideration when choosing the rail steel.

Chen *et al.* (2020) report that the most common properties considered for the rail steel are strength, hardness, fatigue resistance, wear resistance and fracture toughness. The increased stresses from the high-speed of railway transportation cause stress on rail and deteriorate operating conditions. Meyer *et al.* (2018), studying the deformations occurring in railway lines, have determined that most of the occurring deformations are caused by the accumulation of large shear strains close to the rolling contact surface which changes the material behaviour. Considering the conditions that the steel rail is subjected to, Longa *et al*. (2020) agree that the enhancement of mechanical properties extends service life of rail steel. They claim that the new bainitic rail steels recently developed have very strong mechanical properties.

Recent studies have also shown that embrittlement can be a problem that compromise the life of railway lines. The effect of the embrittlement characteristic in rail steel is caused by the hydrogen which is largely produced during the operation of the railway system. Li *et al*. (2016) report that the steel loses its ductility and strength when hydrogen diffuses to the

rail steel grain boundaries. This, in turn, affects the service life of the rail material. As railway steels are always subject to various loads that can initiate fatigue cracks, the material used in rail steel should withstand these kinds of failures. Yet embrittlement tends to affect this material property. Godefroid *et al*. (2020) have recently conducted a study looking at the replacement steel that can be used in railway lines (C-Mn-Si common steel vs Nb-V-microalloyed steel). While the two steels have similar properties, the microalloyed steel outperforms common steel when it comes to resistance to abrasion and fatigue crack growth; hence, microalloyed steel has been a recommended candidate for railway lines construction.

Manufacturing process is one of the critical steps requiring extra care when certain properties are required from the material. Railway line steel is one of the materials required to possess certain properties due to the line operational conditions. Qiu *et al*. (2019) insist it is imperative to control steel cooling processes during the manufacturing stage. The proper control of this stage could lead to the attainment of uniform refined intergranular microstructures which can improve mechanical properties. The improved mechanical properties could result in an enhanced performance under various detrimental factors like change in weather conditions and loads. Likewise, Molyneux-Berry *et al*. (2014) are also in agreement that using a proper cooling system during the manufacturing process of the steel is vital, suggesting that controlled cooling also influences the spacing of the pearlite lamellae and gives a smaller spacing which result in a higher hardness.

2.2 Impact of temperature on mechanical properties of rail steel

Temperature influences hardness of the rail steel primarily on the surface where the wheel is making contact with the rail. It is important that the relationship between the rail and wheel is taken into consideration during the manufacturing of rail steel to ensure safe and economic operations of the rail vehicle.

Wang *et al.* (2007), in an experimental study of the impact toughness of rail steel on welded joint at low temperatures, have measured the U-notched and V-notched impact toughness of U71Mn and U75V rail steels from +20℃ to-60℃. The results demonstrate that the impact toughness of rail steel decreases significantly with temperature. Impact toughness decreases at low temperatures and brittle cracks occur more easily on the welded joints. They observed that U71Mn rail steel has higher impact toughness than U75V rail steel from −60 to +20°C.

Hu *et al.* (2020), from their study examining the wear and rolling contact fatigue of materials, report that increasing temperature during loading causes debris which comes from the wheel and sticks to the rail surface, resulting in adhesive wear on the rail surface. Olofsson and Telliskivi (2003) report that high temperatures of rail-wheel contact result from the slip causing thermal softening of material and leading to dangerous wear or causing oxidation if surface damage due to wear is smaller. Wang *et al.* (2016) released similar findings from their study of wear and damage transitions of wheel and rail materials under various contact conditions. Temperature variation may cause trains to derail due to excessive deformation or buckling which develop when the steel is exposed to high temperatures for a prolonged period (Hong *et al.*, 2019).

Sanchis *et al.* (2021) have conducted an experimental study assessing the risk of increasing temperature due to climate change on high-speed rail network in Spain. Their findings show that extreme high temperatures are associated with increased incidences of rail buckles. The impact of high temperatures on rail lines differs between geographical locations. They contend that the entire rail line in southern Europe is exposed to periods of elevated temperatures that can cause severe interruptions due to rail deformation, or in the worst case, rail buckling failures. They further justify that continuous change of temperature due to global warming conditions causes vulnerability to these rail lines.

Ferrant *et al.* (2016) used database failure information to examine the impact of temperature on the rail network in Southeast England. Their theory shows a strong correlation between high temperatures and the number of buckling events. They argue that if the temperature is very high, rail line buckling takes place; this is often caused by the additional energy provided by the rail vehicle when travelling on the rail line. There is evidence that a greater number of temperature-related incidents occur in the summer season before high temperatures reduce significantly. They further recommend that speed restrictions at specific critical rail temperatures are executed to reduce the possibility of rail buckling and to minimise the severity of a consequential derailment. Dobney *et al.* (2010) share similar findings from their investigation of the effects of higher summer temperatures due to climate change on the UK railway network.

Studies by Chinowsky *et al.* (2019) suggest that climate change is also a threat to the rail networks mainly due to projected temperature increases. The increase of temperature plays a role in rail line damages; it makes the line vulnerable to damages during periods in which temperatures exceed operating conditions. Rail steel is designed to operate in a narrow range based on the temperature in which it is originally laid, known as the Design Neutral Temperature. When this temperature is exceeded, the ability of the rail steel to support rail traffic begins to weaken. In extreme heat conditions where temperature increases exorbitantly, expansion and unevenness occur which, if undetected, result in derailment.

The strength and ductility of steel is highly dependent on its chemical composition, particularly carbon content, and structure of the material, as proclaimed by Carroll and Beynon (2005). They indicate that carbon can be decarburised, describing decarburisation as the loss of carbon through oxidation from the surface of steel during the manufacturing process at high temperatures. This results in the surface of the rail having a lower carbon content and consequently the steel surface being softer. Msomi *et al*. (2020) share the same sentiments in their study, that decarburisation reduces

hardness of the material which causes reduction in wear resistance and strength, concomitantly enabling fatigue strength and accelerate crack growth.

2.3 Rolling contact fatigue defects due to temperature variation

Rolling contact fatigue defects are mainly due to excessive shear stresses on the rail-wheel contact interface. These defects are related to wear and tear caused by increasing temperatures resulting from the repeated loads applied on the rail steel during operations which brings fatigue and ultimately, rail failure.

The experimental results published by Ma *et al.* (2017) from their investigation on fatigue crack growth and damage characteristics of high-speed rail at low ambient temperature suggest that temperature influences rail material performance, such as stress-strain, yield strength and ultimate tensile strength, which increase as the temperature decreases. As a result, the fatigue crack growth rate and rolling contact fatigue behaviour are affected by temperature with enhanced brittleness and possibly changed pearlite at low temperature. When the temperature decreases from 20°C to 0°C and even further down to −20°C, stress and strength increase, together with partial pearlite, showing different material structure and distribution at 0°C and−20°C. This may improve the slight decrease of fatigue crack growth rate at the initial phase.

Fang *et al.* (2017), studying fatigue failure mechanism at various temperatures of a high-speed railway wheel steel, have determined that fatigue at temperatures below the Fatigue Ductile-Brittle Transition (FDBT) is relatively a different crack growth rate than fatigue above FDBT temperature. Walters (2014) has defined the so-called *Fatigue Ductile-Brittle Transition* (FDBT) in literature as the point at which the fracture mode of the fatigue cracks changes from ductile transgranular to cleavage or grain

boundary separation. Walters (2014) has shared the same sentiments in literature as Walters *et al.* (2016) when they were investigating the effect of low temperatures on the fatigue of S460 and S980 structural grade base plate material at room temperature and -70°C. The results show that the fatigue crack growth rate decreases with lower temperatures until FDBT, and then it increases again. When the temperature decreases below −20°C, the decrease of metal ductility slightly reduces the adhesion coefficient; that increases friction which causes wear on the rail line (Shi *et al.*, 2018).

Sundh and Olofsson (2011), investigating the effects of elevated contact temperature and severe contact conditions related to contact, contend that as the contact pressure and sliding velocity increase between wheel and rail, the contact temperature increases and leads to an increased rate of damage accumulation by ratcheting. This causes a significantly increased wear rate and propensity for crack propagation.

Rolling contact fatigue property and failure mechanism of carburised 30CrSiMoVM steel at elevated temperature were investigated by Wang *et al.* (2016). The results of the worn surface observations of the carburised layer at different temperatures (low –40°C and high –100°C) show that at high temperatures, rail steel develops dent failure whereas at low temperatures, the carburised layer is damaged by delamination. The failure of the carburised layer changes from delamination to dents as the temperature increases. There is evidence that high temperature reduces the RCF life of the carburised steel.

Fang *et al.* (2020) have recently conducted a comparative study of fatigue crack initiation and propagation behaviours at various temperatures. The transition temperature was 40°C for the fatigue test under constant stress amplitude, and for the fatigue under alternating stress amplitude, the transition temperature was 0°C. Observations indicate that as the temperature increased under the constant stress amplitude, the fatigue lifetime decreased. At the alternating stress amplitude, the results show that

fatigue life is not sensitive to the testing temperature. Their finding demonstrate that main cracks tend to initiate from internal inclusions whereas secondary cracking mostly initiate from the smooth surfaces.

Lewis and Olofsson (2009) report that stage 3 cracking is entirely driven by the bending and shear stresses introduced by wheel-rail contact loading, which results in change in temperature and residual stresses. Other small cracks which cannot be shaved, or which wear off grow to a critical size, branching and deepening. Cracks can initiate as a result of white etching layers which result from modification of the microstructure of the rail surface material from pearlite to martensite. White etching layers normally occur because of high temperatures which originate from the wheel slides, if the stress along the front of the crack is equal or greater than fracture toughness of railway material, the crack extends, and the railway line breaks. During the first two stages, the crack grows at an inclined angle with the running surface of about 10-40 mm, and at the last stage the crack first grows with the running surface of about 60-80mm then vertical and break.

Kang *et al*. (2021) discovered that temperature of rails increased between 4.7 K and 12.8 K, the maximum increases for individual rails, in the first 10 h. Under transverse load, the fatigue crack initiated at the rail foot edge on the opposite side of the load application. Subsequently, the cracks propagated along the edge of the rail foot. The rail lines loaded in the transverse direction experience significant fatigue strength but endure fewer load cycles than those loaded in the vertical direction, but over and above, the rails experience larger stresses at the edge of rail foot than in the centre of rail foot under cyclic wheel loads.

Nejad (2020) claims that the difference between the bias temperature and the operating temperature causes thermal stresses, affecting the rail steel fatigue life. The periodic overload needs a highest consideration fatigue life extension. The experimental results show that fatigue life is directly

proportional to the number of periodic overloads applied. Fatigue life reduces after tensile overloading and unloading at the created plastic zone.

2.4 Impact of temperature variation on rail steel performance

Rail steel has been a great challenge for the wheel and rail to operate under different temperatures due to weakening of mechanical properties of steel which increase the risk of material damage and failure. An increase in temperature causes expansion and a decrease causes contraction on the rail steel, which can bend or break. The change in temperature of the rail directly influences the rail thermal properties – stress and force.

Zhou *et al.* (2020) recently investigated the wear and damage behaviours of hypereutectoid and eutectoid rail steels at room temperature and at -40 °C (low temperature) using a rolling-sliding wear test machine. The results show that temperature has influence on the wear and damage behaviour of wheel and rail materials. Moreover, results show that surface damages, which appeared as surface cracks, were observed at room temperature on both kinds of rail steel, whereas at the low temperature, the surface damages of the same steels appeared as small surface cracks and oxide spots.

The hypereutectoid steel presented favourable results of wear resistance at both temperatures – room temperature and low temperature – and a better RCF at room temperature but unfavourable RCF under low temperature. Wear resistance and RCF, however, were both favourable for the eutectoid steel at both temperatures. Wheel and rail materials show smaller wear at –40°C compared to 20°C and smaller damage was observed at 20°C than at –40°C. These views are supported by Zhou *et al*. (2021) who discovered similar results when testing the wear and damage of rail-wheel steels under alternating temperature conditions. They determined that the change in temperature influences the rail and wheel wear of material: the wear rate of

the material at –40°C was three times lower than at 20°C, but the wear rate of the rail material at –40°C was slightly lower than at 20°C. They also indicate that temperature change and humidity have significant influences on the wear and damage behaviours of rail-wheel materials, as they cause oxidation on rail-wheel surfaces.

High temperatures cause expansion on the rail line, increase in stress and buckling. When the train travels faster, it can be difficult to respond to the rail failure, which is why speed restrictions are forced during high temperatures until they drop in the early evening to reduce the probability and severity of rail derailments due to track failure. Low temperatures cause the track to contract and tension cracks to occur (Chapman *et al.*, 2008).

Ma *et al.* (2018), studying wear and damage behaviours of U71Mn rail material and ER8 wheel material under different temperature conditions using a rolling-sliding wear testing device, determined that the wear rate of these materials at room temperature is lower than that at low temperatures. At the same time, the wear rate shows a mild decrease with the temperature reducing from −15°C to −40°C, which is related to the wear mechanism and material properties under low temperature conditions.

Wu *et al*. (2017), from their analysis, have discovered that there is always a temperature difference between the wheel and the rail due to the heat generated by the contact friction during loading. Alternatively, the wheel is always at a higher temperature than the rail material area that comes into contact with the wheel. The rail is exposed to environmental temperatures and therefore is always experiencing thermal shock. The wheel temperature gradually increases as the train is moving, until it reaches a constant temperature where the heat transferred by means of conduction from the contact is the same as the one dissipated. The massive train kinetic energy is transformed into thermal energy due to sliding. Asih *et al.* (2012) propose that the temperature caused by the sliding contact between wheel and rail has been suspected to cause wear. The frictional force caused by rail-wheel

contact during operation raises the temperature that is causing thermal stress and changes the rail material strength, creating thermal softening. After the railway vehicle has passed, the rail cools down to the environmental temperature and the strength of the rail material returns to the previous condition. However, as the temperature increases, thermal stress and thermal softening may occur which can reduce the strength of rail material and make the material more vulnerable to wear (Lian *et al.,* 2020).

Alonso and Gime´nez (2008) recommend that the most important function in railway operation occurs between wheel and rail; it is assumed that temperature plays a significant part in this area. Heat transfer occurs on the wheel and rail and heat exchange occurs on the surface between wheel and rail and surroundings after the rise of temperature. The rail steel has a tendency to vary in length due to the increase or decrease in temperature. The effects of expansion or contraction depend on the rate of change of temperature of the material (Bird & Ross, 2014).

Vo *et al.* (2015) have investigated the wheel-rail contact condition to determine the temperature rise due to high adhesion contact and thermal influence on wear and rail life using a three-dimensional (3D) elasto-plastic finite element model. The results show that the residual heat of the first wheel passing on the rail, combined with the heat produced by the next wheel passing, results in an increase of temperature that can reach critical value of +720°C. This is the temperature at which the white etching layer begins to form, and plastic deformation continues to accumulate until the ductility of the material is exceeded and the rail ruptures. Vo e*t al.* further explain that if the temperature at the contact zone surpasses 2501°C, the yield strength reduces.

2.5 Impact of change of weather conditions on rail steel behaviour

Extreme weather conditions, even though they occur in the shorter term, have an impact on the railway transport and its management. Rainfall, high temperatures, cold snaps, high winds and snow all cause operation disruption and damage rail lines. During heavy rainfall, rails become slippery and train drivers are required to apply breaks at a far distance to ensure a safe standstill; this accelerates the rolling contact fatigue damage.

Rossetti (2002) reports that if railway lines are exposed to extreme cold weather conditions (although not applicable in South Africa), railway lines freeze and become brittle, increasing the risk of railway line fracture. Climate change also has an impact on damaging railway lines because when these are exposed to sunny weather with high temperatures, they occasionally develop heat curves that cause thermal expansion. Uneven thermal expansion causes misalignments on railway lines that are often identified as a cause of train derailment, potential accidents, injuries, fatalities, property damage and toxic release of dangerous materials of which a train is comprised.

Mirkovic *et al*. (2021) have claimed that rail temperatures are affected not only by the air temperature but also by other climatic parameters such as wind, rain, sun and cloudiness during the day. According to Ekberg and Pålsson (2019), in an open environment, friction characteristics of the wheel-rail can be affected by various third bodies which can be found at the rail-wheel interface. They get entrapped at the rubbing surfaces for a period. The third bodies can be sanding particles, natural contaminants such as leaves, anti-freeze, water, snow or wear debris of wheel and rail formed during rolling-sliding. In addition, Wang *et al*. (2021) report that Arias-Cuevas found that excessive sanding particles potentially lead to electrical insulation of rail-wheel contact which can cause the failure of the rail vehicle detection system.

Koetse and Rietveld (2009) contend that cold weather conditions impact railway structures in a way that changes the material properties of the railway line and increases degradation rate. Frost in counterweight and substructure affects the global stiffness; therefore, the fracture toughness of railway line steel changes with temperature and can damages the railway line.

Thaduri *et al*. (2020) have discovered a rarely considered point in research on space weather. This is one of the extreme climate changes that could potentially also threaten railway infrastructure. It is described as a branch of space physics and aeronomy, or Heli physics, concerned with the time varying conditions within the solar system, including solar wind, emphasising the space surrounding the earth, including conditions in the magnetosphere, ionosphere, thermosphere and exosphere. Railway infrastructure may be negatively affected by the extreme space weather events which can be due to effects on system components driving the whole rail system such as electronic components built in signalling systems.

Bansal *et al.* (2019) suggest that brakes applied for a prolonged time raise the temperature of the wheel tread and rim of the rail. This may cause cracks and increase its growth rate. Sudden braking also has a major impact on temperature changes as temperature almost doubles if trains are brought to rest under emergency braking.

Burroughs (2019) and Fu *et al.* (2019) share the same views about the effect of climate change on the railways system. Railways are always affected by different climatic events which impact its operations. Extreme climatic conditions such as storms, heavy rains, sun and snow disturb the rail performance, including colder winters or hotter summers or unpredictable extreme weather condition. All these increase the risk of damage to critical railway infrastructure and assets and frequently endanger safety and punctuality requirement.

2.6 Factors transforming microstructure of rail steel

Microstructure controls the behaviour of mechanical properties of rail steel. Most rail steels are comprised of eutectoid steel with a fully pearlitic microstructure as pearlite provides the best mechanical properties. Changes of temperature influences these properties. Various microscopy methods are used to characterise the effect of the microstructure on the mechanical behaviour; the effect is determined by the grain size, structure or content distribution.

According to Mitao *et al*. (2002), microstructure of rail steel is comprised entirely of pearlite which consists of a mixture of relatively soft ferrite and hard cementite. The rough parallel plates in a lamellar of railway line steel structure are formed by ferrite and cementite. This structure of rail steel creates good wear resistance due to hard carbide and a degree of toughness because of ferrite's ability to flow in an elastic/plastic manner. However, during operation, rolling contact friction which generates heat commonly causes microstructure transformation on the rail surface (Chen *et al.,* 2019). Meyer *et al*. (2018) also report similar views that railway rails are mostly made of carbon steel with a pearlitic microstructure. Due to high rolling contact loads to which the surface layers of wheel and rail are subjected during their service life, these building blocks provide an equitable trade-off between cost, wear and strength.

Railway line steel with small pearlite interlamellar spacing is assumed harder and tougher. Atroshenko *et al*. (2020), in a study on the fractured certain steel rail, discovered that fracture is divided into three stages: initial fracture stage, intermediate fracture stage and end fracture stage. The structure of the initial fracture stage still shows lamellar pearlite with fine grain; structure of an intermediate stage shows the crack begins to form from clusters of non-metallic inclusions elongated during rolling, with microcracks located near the fracture surface; and lastly, at the end fracture stage, there is deformation with a branched network of microcracks, the

structure showing a mix of components, crystalised and increased pearlite grain size. These findings are the same as those published by Msomi *et al*. (2020).

Maruyama *et al*. (2001) confirm that in rail steels, pearlite is an important feature of the microstructure, apparently achieving a high resistance to wear because of the hard cementite and its restriction by the more plastic ferrite. Consequently, carbon is an essential alloying element. However, it is not only the amount of pearlite that is important but also its shape and the distance between the cementite lamellae. The interlamellar spacing of pearlite is an important microstructural parameter for steels containing pearlite and increases in importance as the pearlite content increases towards a fully pearlitic microstructure. The finer the structure of pearlite, the higher its strength whilst still retaining reasonable toughness. Subsequently, pearlite interlamellar spacing and rail hardness have an inverse relationship. The shorter the inter lamellar spacing, the higher the hardness, wear resistance and tensile strength of the rail steel.

Chen *et al.* (2016), experimenting on rail steel using different cooling rates, determined that when decreasing cooling temperature, the interlamellar spacing of pearlite decreases; this takes place during the pearlite transformation occurrence. The decrease in interlamellar spacing of pearlite increases hardness of the steel. During heat treatment, conductivity limits the size of components that can be produced with the desired microstructure, since transformation depends on the cooling rate and temperature.

Mishra and Singh (2017) explain that various researcher have attempted to clarify the relationship between the fracture toughness of pearlite with microstructural features such as prior austenite grain size, pearlitic nodule size, pearlitic colony size as well as interlamellar spacing. Studies show that fracture has a closer relationship with the pearlite nodule size than the prior austenite grain size. In pearlitic steel, the fracture toughness initially

decreases with decreasing of interlamellar spacing, whereas a complete brittle fracture surface develops when the lamellar spacing is too wide.

According to Athukorala *et al.* (2016), in a study on ratcheting and microstructural characterisation of the rail head, interlamellar spacing strongly correlates with the cyclic softening and hardening of the head hardened rail steel. Samples also show a heterogeneous property of material. When the samples of wheels are subjected to rolling contact tests, samples show an increased tendency to reach rolling-contact fatigue failure prematurely due to high ratcheting rates. Chaves *et al*.'s (2020) study concluded that a decrease in the pearlite formation temperature leads to a reduction of the pearlite interlamellar spacing while increasing hardness. They also observed that pearlite interlamellar spacing reduction enables a better wear resistance performance in sliding wear tests.

2.7 Summary

The literature shows that while railway line material is a strong material, it is evident that temperature plays a significant role in influencing the rail line material when in operation. Researchers detect a strong correlation between temperature variation and certain problems occurring on the rail steel material. Elevated temperatures cause buckling failures on the rail line whereas low temperatures cause the steel to contract. This change of temperature on rail steel causes severe operation disruption and damages rail lines. It is apparent that temperature is another significant factor affecting microstructure of the rail steel. The rail steel microstructure transforms and becomes brittle due to temperature change which then leads to increased wear, reduction of material strength and fatigue failures which potentially increase crack growth rate and, in the end, reduce rail steel material life span. In some areas, speed restrictions are implemented to diminish the likelihood of rail buckling and to minimise the severity of a consequential derailment.

Numerous studies throughout many countries have investigated the impact of temperature change on rail line steel. It is evident that temperature, due to its variation, is a primary factor causing severe damages on rail line steel. In spite of this, many researchers still feel that more research in this area is required. However, as there has been little attention on South African rail lines, the purpose of this present work is to determine the impact of temperature variation specifically on South African rail line steel.

CHAPTER 3

EXPERIMENTAL SETUP AND PERFORMANCE

3.0 Introduction

This chapter presents a discussion of materials and equipment used in fatigue experiments conducted for this study to determine the change in the microstructure of the rail line steel when a load is applied repeatedly. This chapter also provides in-depth information on microstructure tests performed on fatigue tested samples and equipment used to achieve the results.

3.1 Experimental setup

The following list contains the equipment used in conducting the experiments for the study:

- Instron 8801 Servohydraulic Fatigue Testing System
- Struers LaboPress-3 Thermal Compression Moulding Machine
- Struers LaboPol-5 Polishing Machine
- Innova Test Falcon 505 machine-hardness tester
- Inverted Metallurgical Microscope, AE2000 MET
- Scanning Electron Microscope (SEM) Analysis with Energy Dispersive X-ray

3.2 Description of equipment

This section briefly describes each piece of equipment used in conducting various tests and experiments for this research.

3.2.1 Instron Machine 8801 Servo-hydraulic Fatigue Testing System

The 8801 Fatigue Testing System is a servo-hydraulic testing system for static and dynamic testing with a large workspace, rigidity, precision alignment and a capacity of up to 100 kN.

Figure 3.1: Instron Machine 8801 - Fatigue Testing System

3.2.2 Struers LaboPress-3 Thermal Compression Moulding Machine

Struers LabroPress-3 Moulding Machine is an automatic electro-hydraulic metallographic mounting press with 32mm mould cylinders diameter, 40mm diameter securing cap, water cooling supply and drain. It has temperature, force, and time (heating and cooling times) setting parameters for monitoring compressed samples.

Figure 3.2 Struers LaboPress-3 Thermal Compression Moulding Machine

3.2.3 Struers LaboPress-5 Polishing Machine

Struers LaboPress-5 is a manual and semi-automatic grinding and polishing machine used in the lab with variable speed up to 400 rpm and 250 mm diameter disk size. Holding three samples at a time, it has an automatic water valve, manual splash guard and bowl liner. Its endurance and speed keep up with 24/7 throughput, enabling faster and more reliable preparation of specimens.

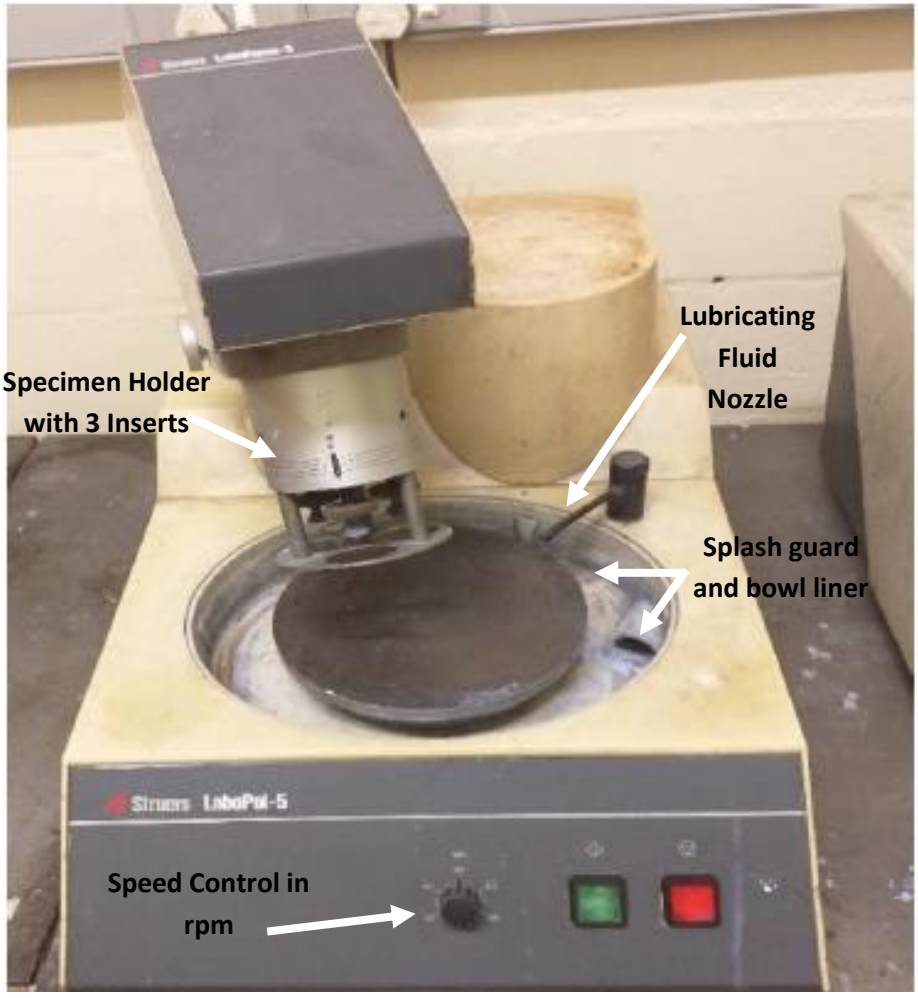

Figure 3.3: Struers LaboPress-3 Thermal Compression Moulding Machine

3.2.4 Inverted metallurgical microscope, AE2000 MET

This is a Light Optical Microscope with specifications of coaxial coarse and fine focus, five-fold nosepiece and a complete series of LM plan achromatic objectives. It is designed for inspection of bulk samples, mostly used in the steel industry. It can inspect large pieces and die casting for failure analysis, material research and quality control. It has high contrast and resolution in bright field as well as dark field, providing excellent images.

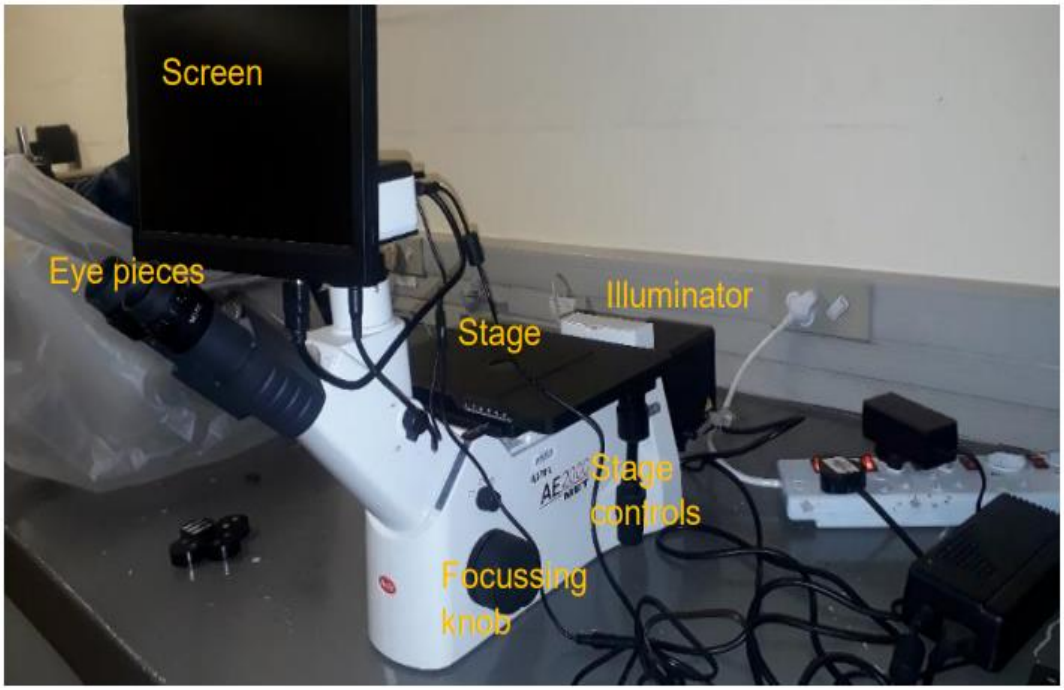

Figure 3.4: Inverted metallurgical microscope, AE2000 MET

Figure 3.5: LM Plan Achromatic inverted microscope objectives: nosepieces

3.2.5 InnovaTest Falcon 505 Vickers Microhardness Tester

This is a hardness tester which indicates the hardness of a material by measuring the effect on a material surface of a localised penetration, using a diamond indenter with a pyramid shape on the tip. It operates with a load of up to 200 kilogram-force for a maximum of 15 seconds.

Figure 3.6: InnovaTest Falcon 505 Machine – microhardness tester

3.2.6 Scanning Electron Microscope (SEM) analysis with energy dispersive X-ray

This is a Scanning Electron Microscope – Tescan Mira 3 of the University of Cape Town – with specifications of 30 kV and the working distance of 12mm max. This instrument is connected to Energy Dispersive X-ray.

A scanning electron microscope (SEM) is a type of electron microscope that produces images of a sample by scanning the surface with a focused beam of electrons. The electrons interact with atoms in the sample, producing various signals that contain information about the sample surface structure and material composition. The electron beam is scanning in a raster pattern, and the position of the beam is joint with the intensity of the image detecting signal. Images are produced by making use of back-scattered electrons and secondary electrons generated within.

SEM used in conjunction with energy dispersive X-ray spectroscopy (EDX) allows measurements of X-rays and gives images at larger depths of the sample. X-rays generated in an SEM are formed through an electron beam which traces the sample, transferring some of its energy to the sample atoms. This energy is used by the electrons of the atoms to move to the high energy shell, leaving a hole with a positive charge which then attracts the negatively charged electrons and fills the hole of the lower energy shell. The energy difference of this transition between high and low energy shells, released in the form of an X-ray, identifies the type of elements that exist in a sample and map the distribution of the atoms.

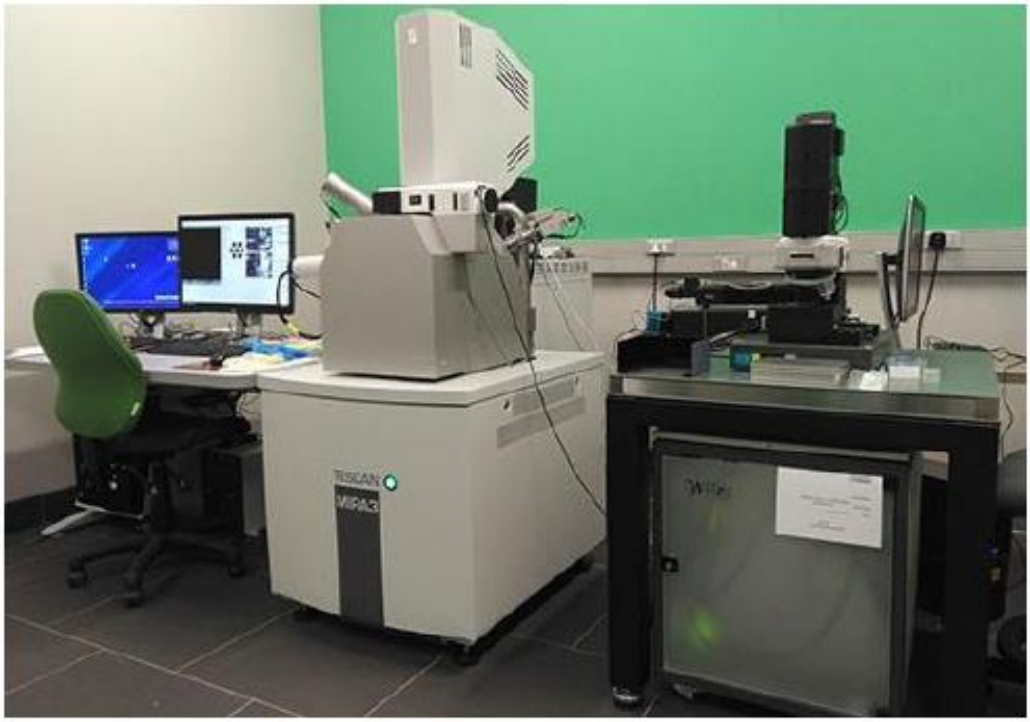

Figure 3.7: Scanning Electron Microscope (SEM) analysis with energy dispersive X-ray from UCT

3.3 Preparation and performance of experiments

This section is focused on the experiment conducted in this study. The sub-sections discuss the details of each step of the experiment. The experiment begins with the preparation of specimens for performing the fatigue test, followed by the actual fatigue test, and lastly, preparation of specimens for analysing experiments.

The experimentation was performed on four specimens. All four test specimens were from new rail material, never before used, and were cut from the railhead along the direction of the rail.

3.3.1 Preparation of specimens for fatigue performance

CNC was used to cut the rail head to 20 mm thick pieces: specimens were cut vertically down from the railway line material piece, hot rolled, high

carbon steel – R900A/R1100 UIC860. Only railhead was used for this investigation. They were then machined on one side using a milling machine to obtain the shape which would fit onto the Instron Machine clamps. Specimen dimensions during the fatigue test were 68 mm X 55 mm X 20 mm (max); irregular shapes (see Figure 3.8 a, b, c). Specimens were cut to fit onto the Instron Machine clamps. The jig to strike specimens was cut from the rail line material since other available materials were too soft.

3.3.2 Performance of fatigue test

Three of four specimens were exposed to a fatigue test on a repeated vertical linear load of 50kN using the Instron Machine (see clamping of specimens in Figure 3.8 d). Each specimen was under the load of 50 kN, but the difference was in times. One specimen was under load for six minutes, another one for eight minutes and the last one for 10 minutes.

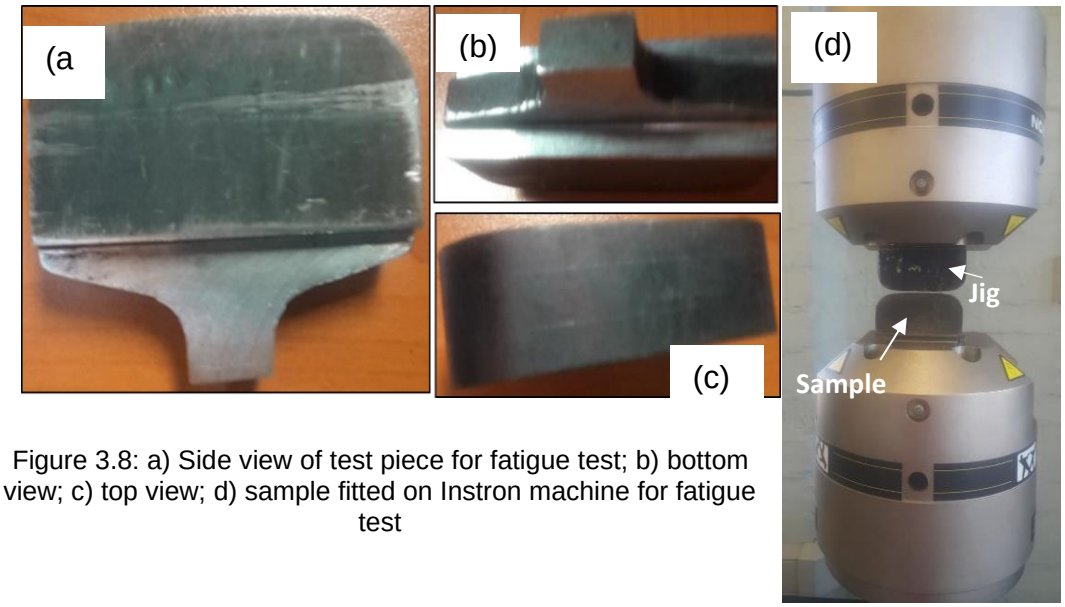

Figure 3.8: a) Side view of test piece for fatigue test; b) bottom view; c) top view; d) sample fitted on Instron machine for fatigue test

3.3.3 Preparation of specimens for test analysis

This section presents information pertaining to specimen preparation. The following sub-sections provide details for each step in the process of preparing specimens.

Specimens were cut with a waterjet machine at Waterjet Technology (Pty) Ltd. Specimens were cut to the size of 25mm x 15mm x 15mm each (see cut-out expression drawing in Figure 3.9 a, b, c). The specimens were fitted into a moulding machine with a diameter of 40mm, surroundings filled with acrylic resin particles and closed at the top with a plunger to apply enough pressure for proper moulding. The mould was heated at 180^{o}C, pressurised at 320 kPa and left to cure for 10 minutes. Then, as the mounted specimens were removed from the mould, they had a beautiful structure (see Figure 3.9 d). This was done for easy handling during grinding, polishing and the microstructure examination process.

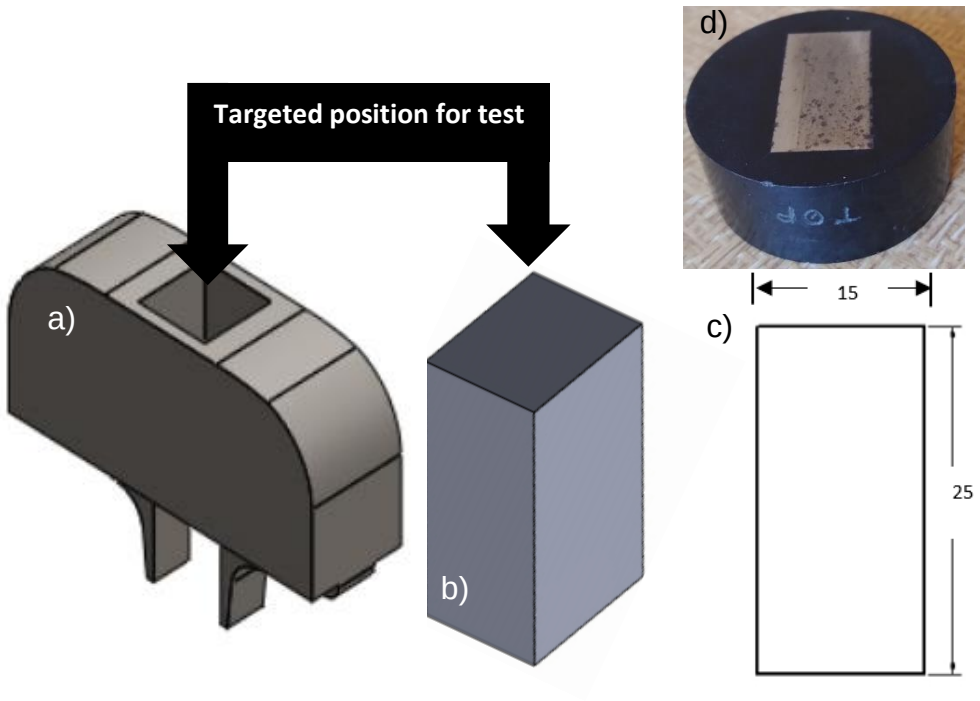

Figure 3.9: Test specimens a) targeted position on rail line head for fatigue test; b) cut-out of specimen; c) specimen dimensions; d) mounted specimen dimensions

Table 3.1 illustrates the materials and chemicals used and the steps followed during the grinding and polishing of specimens.

Table 3.1: Specimen preparation method

Step	Pad	Polishing solution	Lubricant	Speed	Time
Plane grinding	320 grit SiC paper	-	Water	200 rpm	5 min
Fine grinding	1500 grit SiC paper	-	Water	200 rpm	10 min
Fine grinding	4000 grit SiC paper	-	Water	200 rpm	10 min
Polishing	Daran/ Dac	3µm diamond suspension	AKA-Lube/DP-blue	100 rpm	5 min
Polishing	Napal/ Nap	0.2µm OP solution	Water	100 rpm	1.5 min
Rinsing	Napal/ Nap	-	Water	100 rpm	min

3.3.3.1 Grinding process

The specimens had a better surface finish as they were cut using CNC, waterjet and milling machine; however, they did have visible tiny scratches and deep marks.

The appearance of specimens determined the grit size to use first. The first step started with 320 grit SiC paper as the lowest/rough grit abrasive. Specimens were manually held and rotated with their surface against the grit abrasive paper, continually changing the direction from 45 to 90^{o} within the intervals of 30 to 40 seconds.

The 320 grit was followed by 1500 grit, and the desired finish was achieved on fine 4000 grit SiC paper. Between the changing of grit abrasive papers, the machine was flushed, and specimens were rinsed meticulously with tap water to remove loose abrasive particles which can possibly cause scratches on the next step.

3.3.3.2 Polishing process

Specimens were polished on the Struers LaboPol-5 Polishing Machine (see Figure 3.10) using 3µm diamond suspension with AKA-Lube/DP-blue lubricant and 2µm OP solution for 10 minutes and 90 seconds, respectively. After each polishing step, the specimens were rinsed thoroughly with tap water, covered with a small amount of ethanol and dried with warm air from a household hairdryer. This was to avoid oxidation that can occur on the polished surface while changing to the next step of polishing. These polishing steps removed the top layer with tiny scratches and properly prepared specimens for etching and microstructure examination.

a) b) c)

Figure 3.10: Polishing chemicals a) F3µm diamond suspension and AKA-Lube/DP-blue; b) 0.2µm OP solution

3.3.3.3 Etching

After completing polishing, specimens were etched with 3% Nital etchant. This was used to determine microstructure and grain boundaries of the steel. The specimens were immersed in the etchant for eight seconds and then thoroughly rinsed with distilled water. Afterwards, the surface was cleaned with ethanol and then dried with hot air.

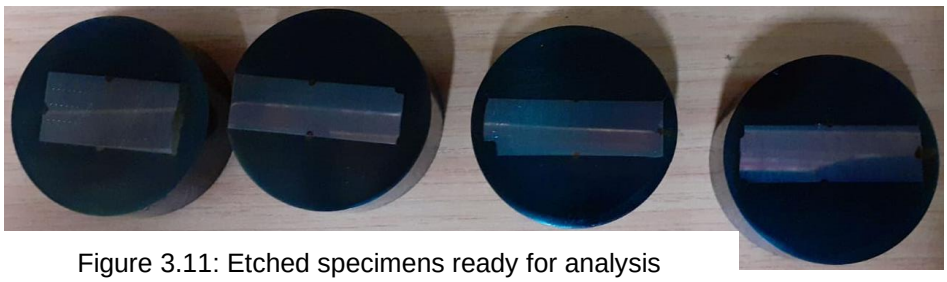

Figure 3.11: Etched specimens ready for analysis

3.4 Microstructure analysis

During the macrostructural analysis, specimens were placed on the flat stage surface of the microscope, facing down to allow the direct nosepiece projection to the targeted surfaces on the specimens without interfering with a mounting resin. LM Plan 10X/0.25 BD and LM 50 X/ 0.55 BD were used to magnify the microstructure images. Grain images were captured through the connection of the monitor to the microscope. This test provided detailed information of material microstructure.

3.5 Microstructure characterisation

This machine depends largely on the detection of high energy electrons released from the sample surface after exposure to a highly focused beam of electrons from an electron gun. This beam of electrons was focused on a small spot on the specimen surface, using the SEM objective lens. It used accelerating voltage and size of hole, and the distance between the sample and working distance was adjusted to achieve the best quality images.

During the analysis of steel microstructure, the machine was set to a working distance of 10 mm, at the resolution scale of 1000µm and magnification of 100kx. During the testing process, chemical compositions across images were captured at an adjusted distance of approximately 30mm using a backscattered electron. An accelerating voltage rate of 20 kV exposed specimen surface features. SEM was connected to the energy dispersive X-ray facilities to determine the chemical elements within the specimens using a 70 and 80 µA filament current.

3.6 Microhardness analysis

A Vickers microhardness test was performed on the same samples used for microstructural analysis using InnovaTest Falcon 505 Machine hardness tester, with a load of 0.5 kilogram-force, interval of 2mm and objective 20x to conduct the hardness testing. The specimens were placed on the machine flat working table, face up, one specimen at a time. The test bed was adjusted to the level of contact with the specimens, and the machine was activated to begin the testing process. Indentation measurements were achieved on the cross-section of the specimens. Three lines of tests were completed on each specimen cross-section. As the machine is computerised, results were recorded automatically.

CHAPTER 4

EXPERIMENTAL RESULTS AND DISCUSSION

4.0 Introduction

This chapter presents the analysis of microstructure results of the rail line steel observed using an optical microscopy (OM) with Scanning Electron Microscope (SEM) and a Vickers Microhardness. The results obtained were for the tests conducted on four specimens, three of which were exposed to fatigue test. Specimen microstructure images were taken from the positions where the fatigue load was applied: the head rail side, the surface which gets exposed to rolling contact when the rail system is in operation. This was to check the impact of fatigue on the material.

4.1 Microstructure results

Firstly, specimen surfaces were properly polished and etched by 3% Nital to easily observe the distribution of alloying elements. The metallurgical structure for specimen surface was observed by a light optical microscope (LOM) and images were captured. Micrographs were taken on low and high resolution to expose the appearance of alloying elements in the steel.

Figure 4.1 shows base material microstructure results: a homogeneous mixture of elements, consistence of grain sizes of different elements, in both high and low resolutions, in black and white. Black represents pearlite while white represents ferrite grain boundaries (Kang *et al.*, 2021). This indicates that the rail steel is strong and resistant to wear when it is in its original state, not subject to any load.

Figure 4.2 shows a slight change in the characterisation of elements. The imbalance of elements is identified in Figure 4.3 where the colour has slightly changed to brown, indicating the solubility of carbon in iron.

In Figure 4.4 the micrograph observations show a continuous ferrite networks and pearlite grains. It was also observed that the grain sizes were rather heterogeneous with weak ferrite. This is the specimen in which fatigue load was applied longer. The observed results show a distortion of grains, elongated and smaller sizes of the pearlite colonies with shorter interlamellar spaces. Unfortunately, they were not quantified. Considering the weaker strength of ferrite distributed like nets compared with pearlite, it can be assumed that cracks on rail steel initiate from the ferrite networks where carbon reduction is observed (Masoumi *et al.*, 2019). The rail steel fails due to repeated alternating stresses from the running rail vehicle. The results obtained in the study confirm that carbon content plays a significant role in strengthening, hardening, and generating resistance to wear in the steel.

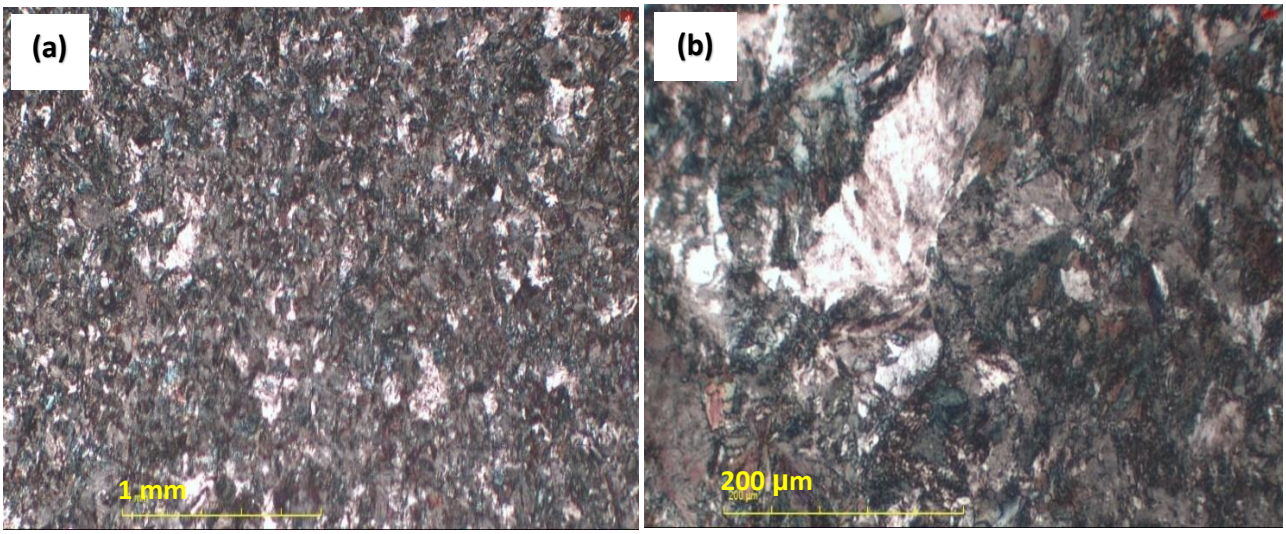

Figure 4.1: (a): Optical Microscope Micrograph – base material (a) at low resolution; (b) at high resolution

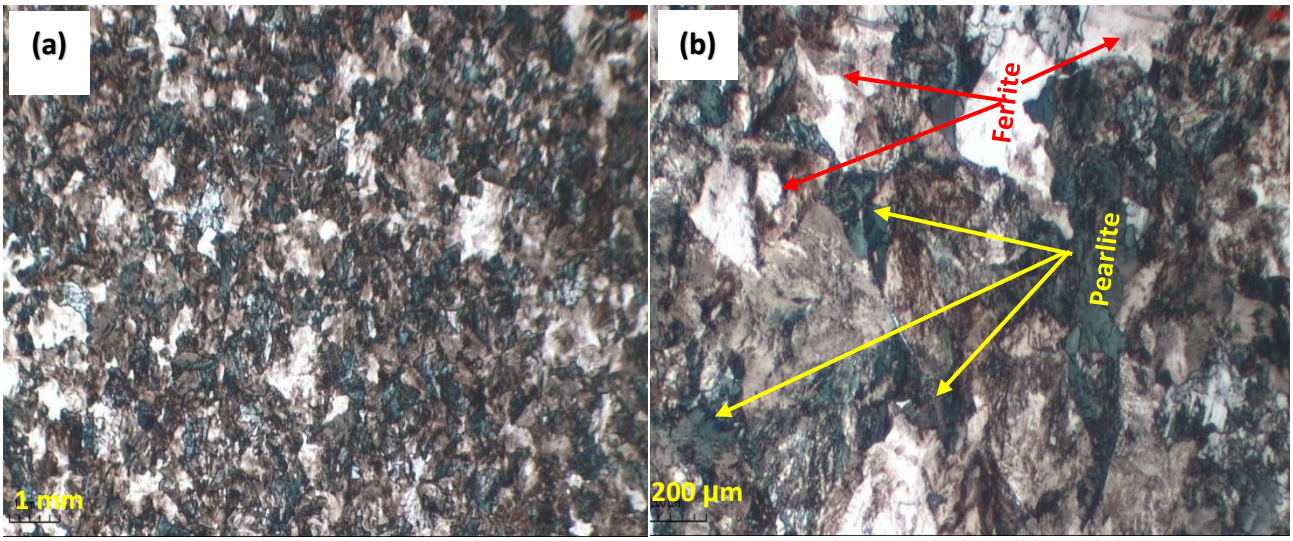

Figure 4.2: Optical Microscope Micrograph – Specimen 1 (a) at low resolution; (b) at high resolution

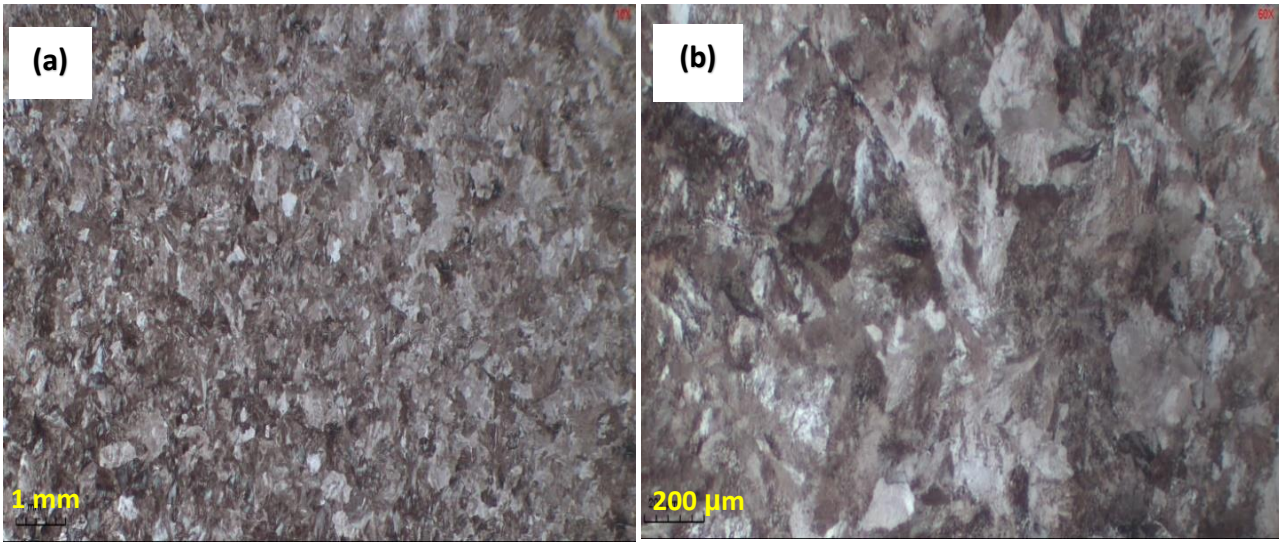

Figure 4.3: Optical Microscope Micrograph – Specimen 2 (a) at low resolution; (b) at high resolution

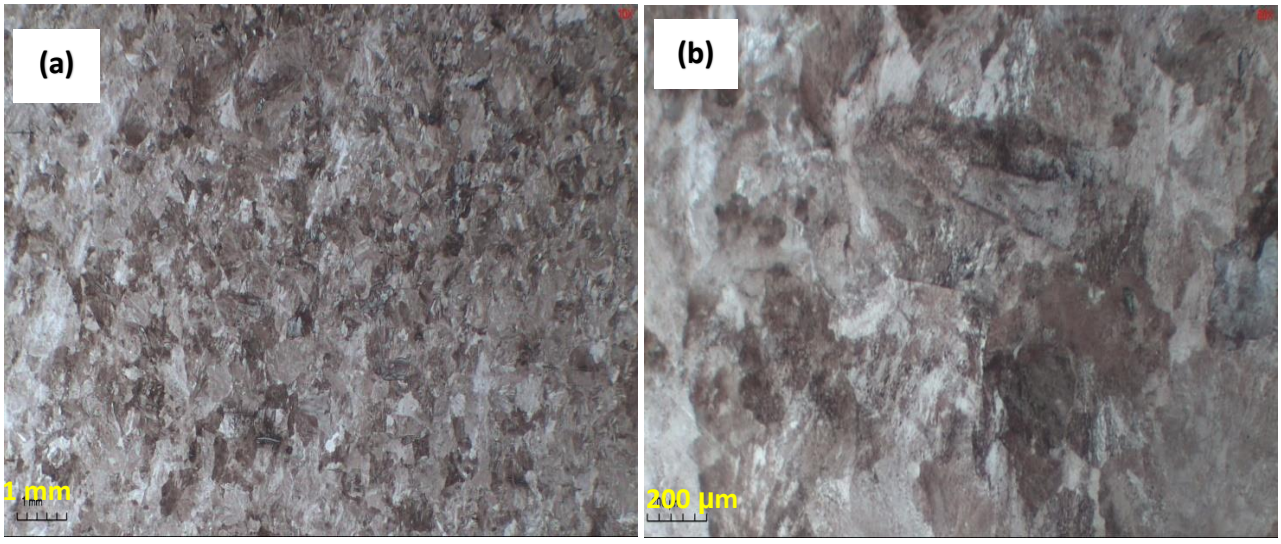

Figure 4.4: Optical Microscope Micrograph – Specimen 3 (a) at low resolution; (b) at high resolution

4.2 SEM microstructure analysis

SEM micrographs in Figure 4.5 (a) to (d) show the microstructure of pearlitic rail steel, presenting lamellar structure of cementite (white) and ferrite (black). The interlamellar spacings look different in all specimens which were placed under load at various intervals. It can be observed that time has influenced the results. If specimens are placed under fatigue load longer, this affects the transformation of grains. By increasing cycle load time, carbon content decreases and caused weakness in the material (Masoumi *et al.*, 2019). Figure 4.5 (a) shows fine thin ferrite grains of microstructure; Figure 4.5 (b) shows a slight grain elongation perpendicular to the direction of fatigue load; Figure 4.5 (c) shows a clear distortion with elongation and reduction of pearlite colon sizes; and Figure 4.5 (d) shows a complete dislocation of grains which confirms an increased amount of deformation due to fatigue. The curvy shapes and curly cementite lamellas have developed from the accumulation of dislocations in the ferrite/cementite interface (Zhang *et al.*, 2020).

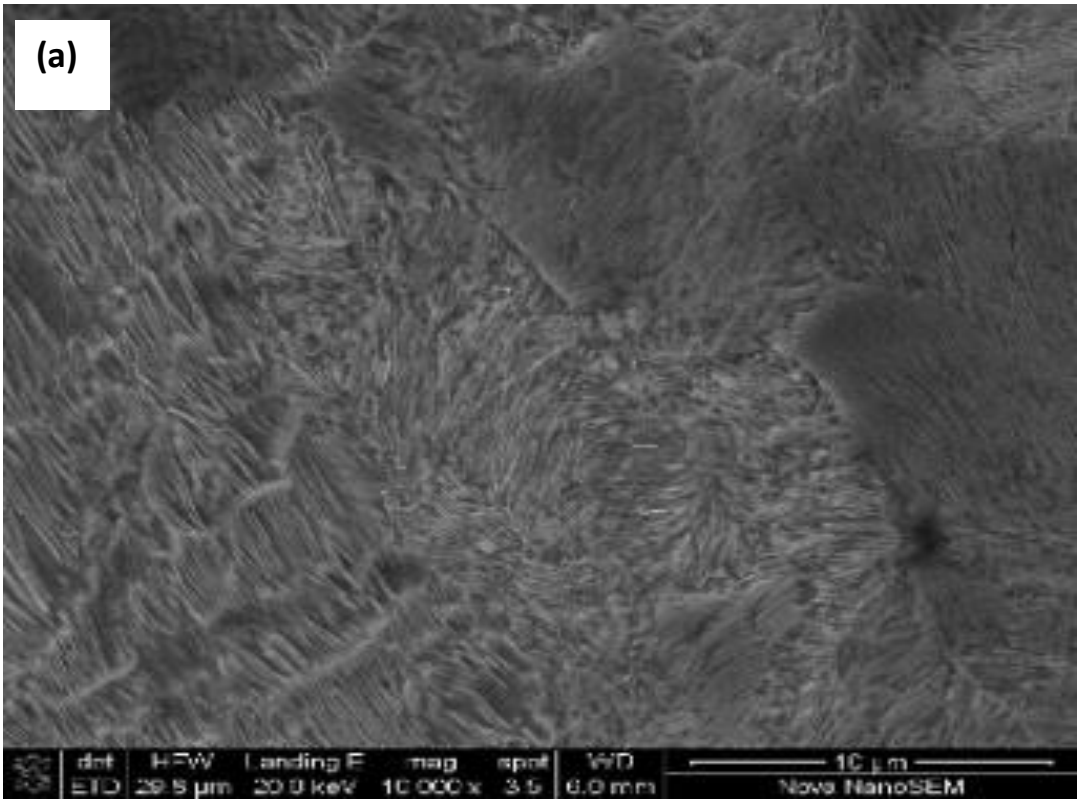

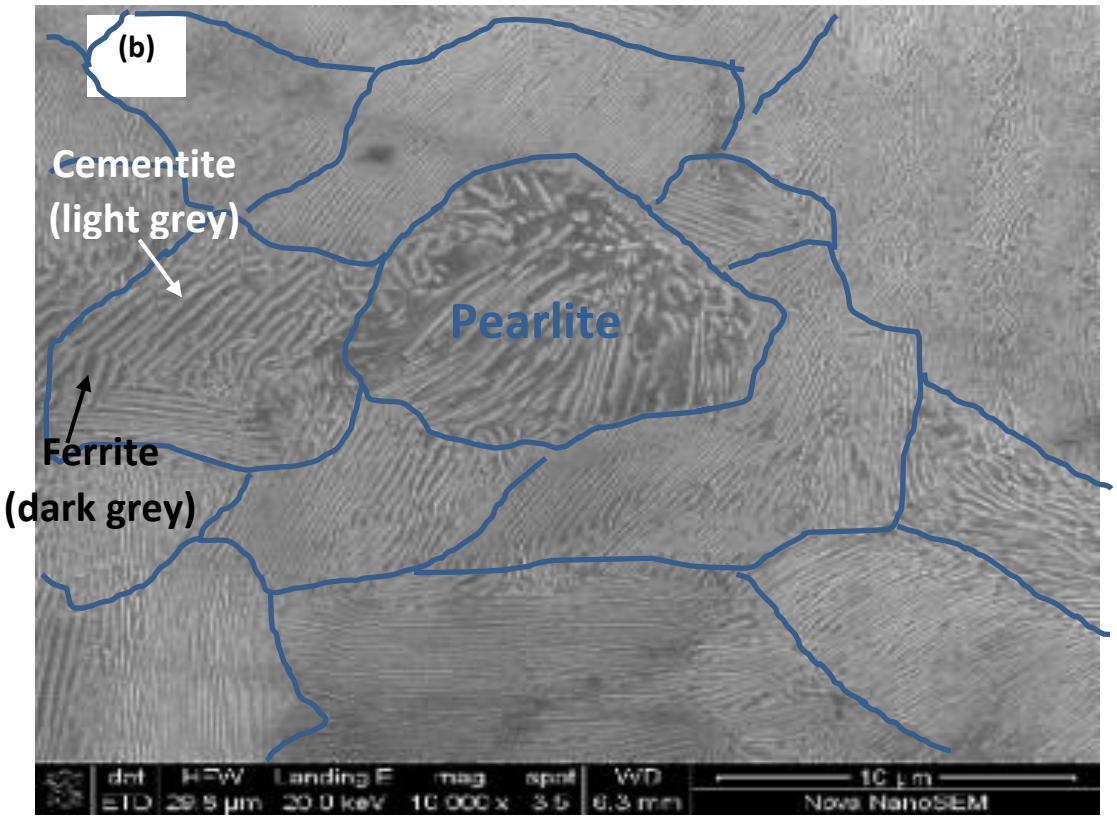
(b)
Cementite
(light grey)
Pearlite
Ferrite
(dark grey)
Nova NanoSEM

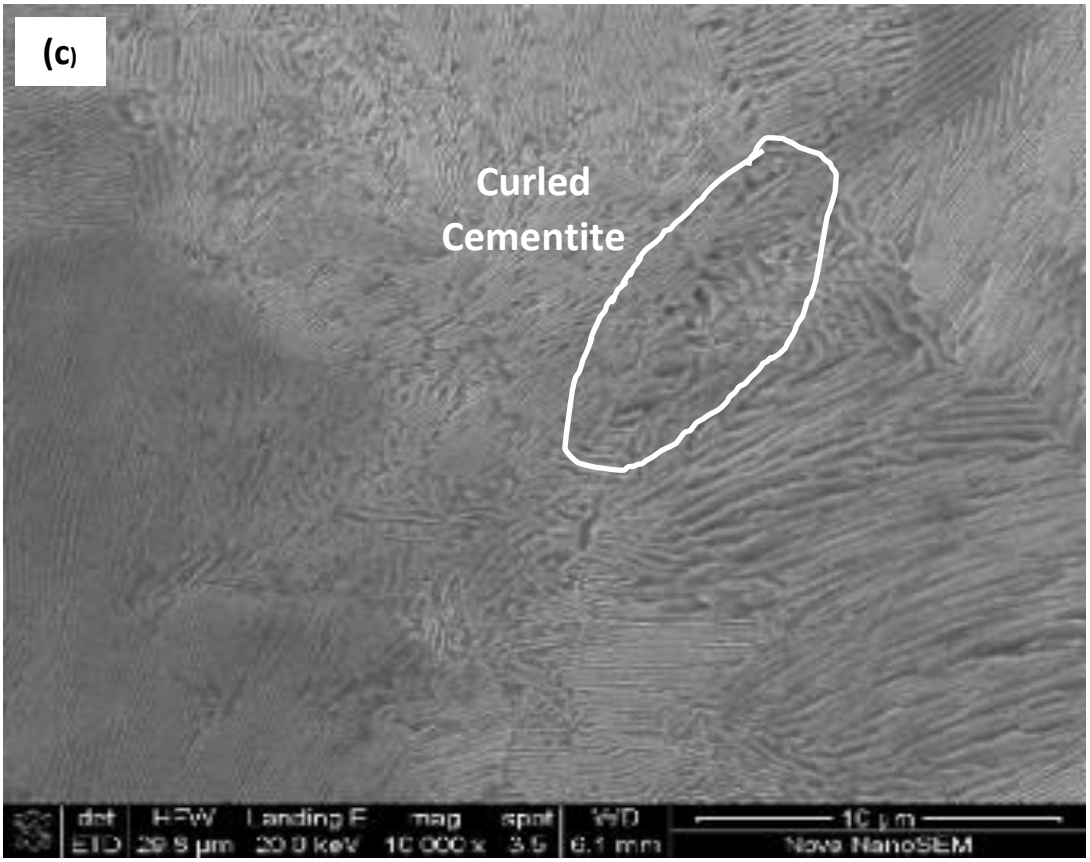
(c)
Curled
Cementite
Nova NanoSEM

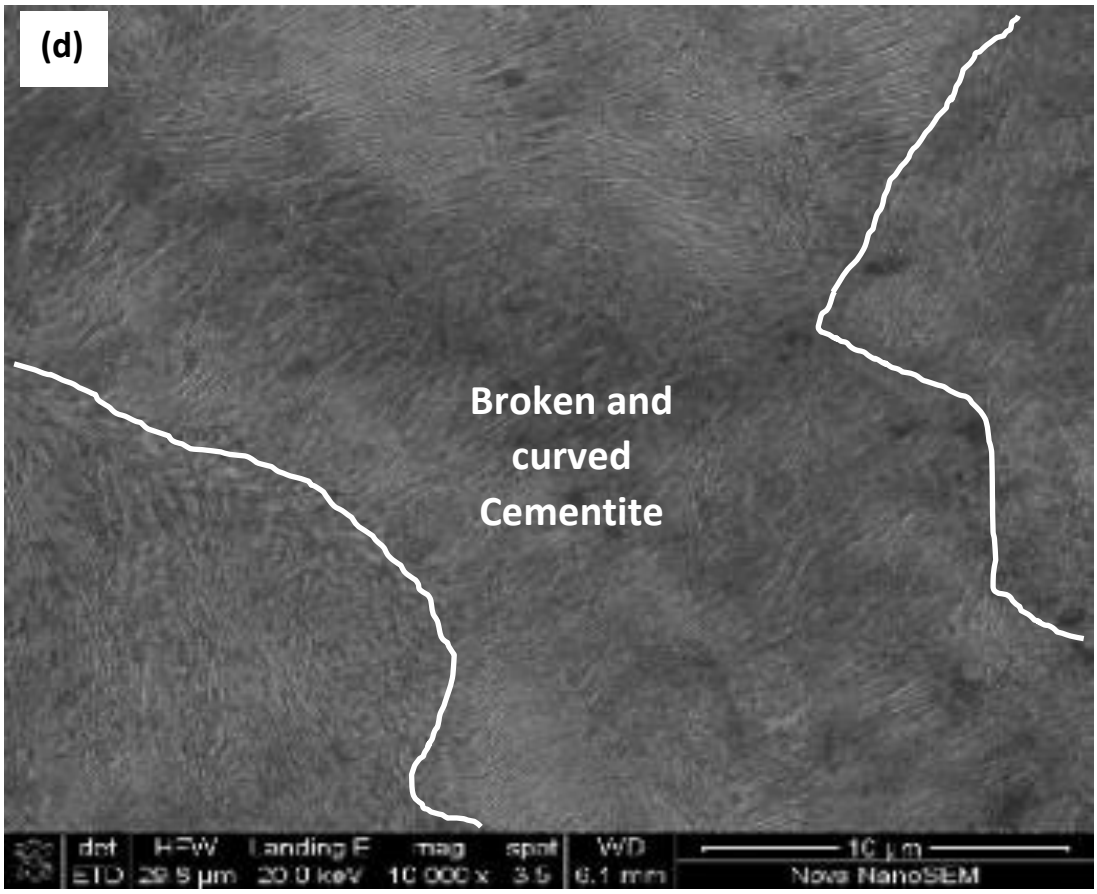

Figure 4.5**:** SEM micrographs of experimented rail steel showing elements transformation: (a) base metal; (b) Specimen 1; (c) Specimen 2 with element identification; (d) Specimen 3 showing clear cementite transformation

4.2.1 Energy dispersive X-ray analysis

Tables 4.1 to 4.4 show chemical composition in percentage by mass of four specimens extracted from the rail piece, three of which underwent a fatigue test. EDXS characterisation of elements is presented in Figure 4.6. The focus is to determine which element is dominating after the application of fatigue load and its effect in the steel. The chemical composition was determined by analysing the average of different sections denoted by spectrum 1 to spectrum 5 on each sample, as shown in Figure 4.6 (a) to (d). The black particles indicate the existence of carbon, and the grey represents ferrite. The results of EDXS characterisation (in Table 4.1) show a standard average of carbon content on base metal sample. The rising of temperature due to fatigue load distributed carbon content and resulted in its reduction,

as illustrated in Table 4.4. The longer the period of loading, the more carbon content diffuses (Jun *et al.,* 2016).

The grey microstructure consists primarily of iron and manganese, ferrite in its cooled condition. Furthermore, EDXS results show that the effect of increasing loading time not only reduces carbon concentration, but also increases brittleness; however, the manganese element is present to control the structure as it handles repeated impact (Jun *et al.,* 2016).

Table 4.1: Chemical composition impurities of a base metal at room temperature

Spectrum	**In stats.**	**C**	**Si**	**Cr**	**Mn**	**Fe**	**Total**
1	Yes	10.55	0	0	1.06	88.39	100
2	Yes	11.8	0.4	0	1.4	86.4	100
3	Yes	14.09	0.46	0	0.63	84.81	100
4	Yes	13	0.35	0	0.96	85.69	100
5	Yes	13.36	0.56	0.32	1.02	84.74	100
Average		**12.56**	**0.354**	**0.064**	**1.014**	**86.006**	**100**

Table 4.2: Chemical composition impurities of Specimen 1 at room temperature

Spectrum	**In stats.**	**C**	**Si**	**Cr**	**Mn**	**Fe**	**Total**
1	Yes	6.41	0.41	0.00	0	93.18	100
2	Yes	8.16	0.63	0.00	1.07	90.14	100
3	Yes	8.75	0.39	0.00	1.49	89.37	100
4	Yes	7.55	0.71	0.37	1.17	90.21	100
5	Yes	8.78	0.00	0.00	1.35	89.87	100
Average		**7.93**	**0.43**	**0.07**	**1.02**	**90.55**	**100**

Table 4.3: Chemical composition impurities of Specimen 2 at room temperature

Spectrum	In stats.	C	Si	Cr	Mn	Fe	Total
1	Yes	8.52	0.58	0.47	1.09	89.34	100
2	Yes	7.39	0	0	0.84	91.77	100
3	Yes	8.09	0.51	0	1.24	90.16	100
4	Yes	7.76	0	0	1.14	91.1	100
5	Yes	7.43	0.58	0	1.19	90.79	100
Average		**7.84**	**0.33**	**0.094**	**1.1**	**90.63**	**100**

Table 4.4: Chemical composition impurities of Specimen 3 at room temperature

Spectrum	In stats.	C	Al	Si	Cr	Mn	Fe	Total
1	Yes	6.31	0.47	0.53	0	1.54	91.15	100
2	Yes	7.41	0	0.68	0	1.42	90.49	100
3	Yes	5.66	0	0	0	1.46	92.89	100
4	Yes	8.64	0	0.69	0	0.97	89.69	100
5	Yes	7.86	0.44	0.64	0.41	1.09	89.56	100
Average		**7.18**	**0.18**	**0.51**	**0.08**	**1.30**	**90.76**	**100**

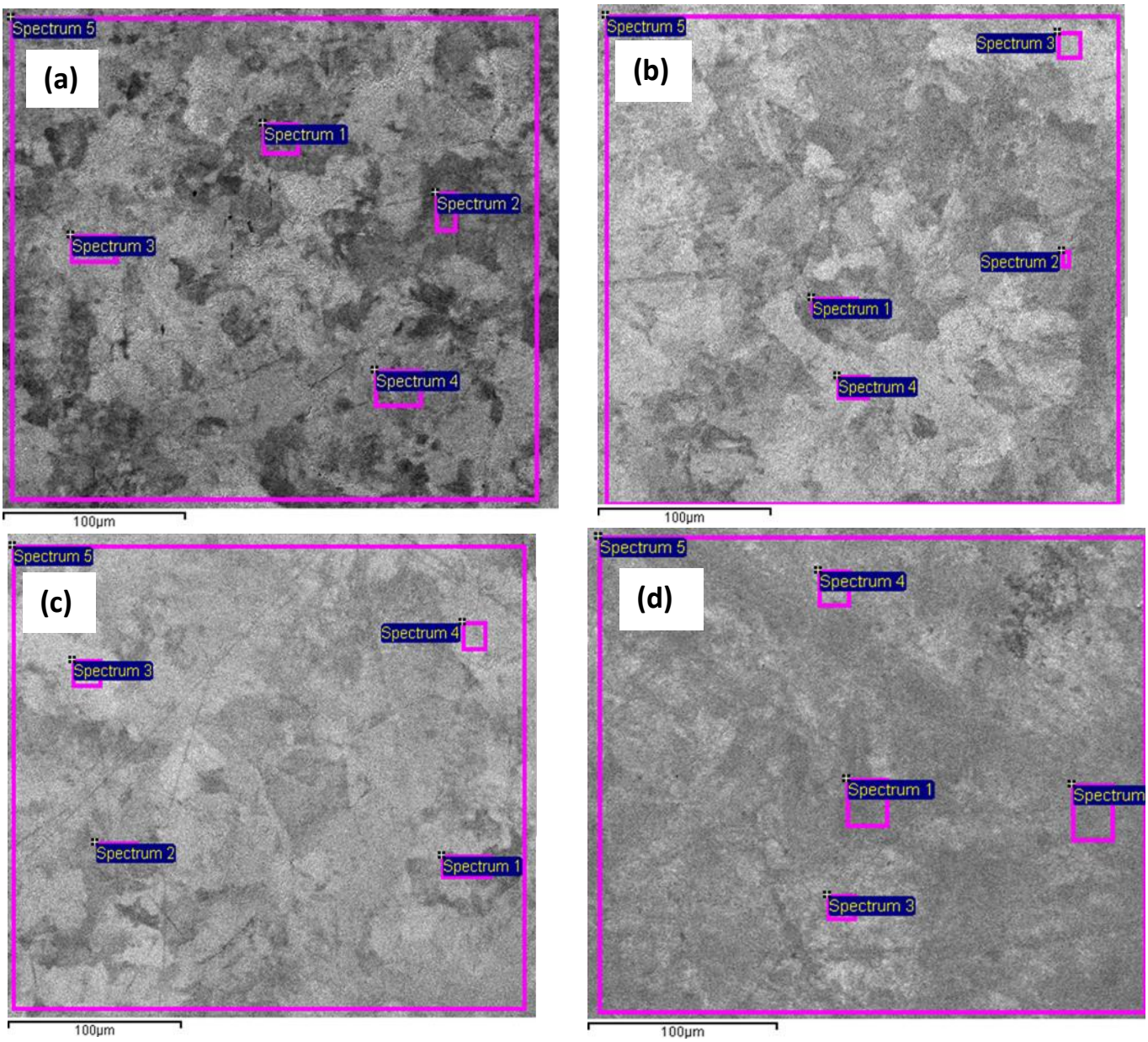

Figure 4.6: EDXS analysis (a) base material; (b) Specimen 1; (c) Specimen 2; (d) Specimen 3

4.2.2 Energy dispersive X-ray spectrum analysis (EDXS)

X-ray continuous and characteristic spectrum is shown in Figure 4.7. EDXS of a rail line steel was carried out at room temperature, with results indicating the presence of carbon, manganese, aluminium, silicon, chromium and iron phases. EDXS has recorded sharp short wavelengths of iron and manganese and identified a wide continuous wavelength of dislocated carbon content which is a good correlation with the SEM and hardness and microscopic observation of microstructure (Masoumi, 2018).

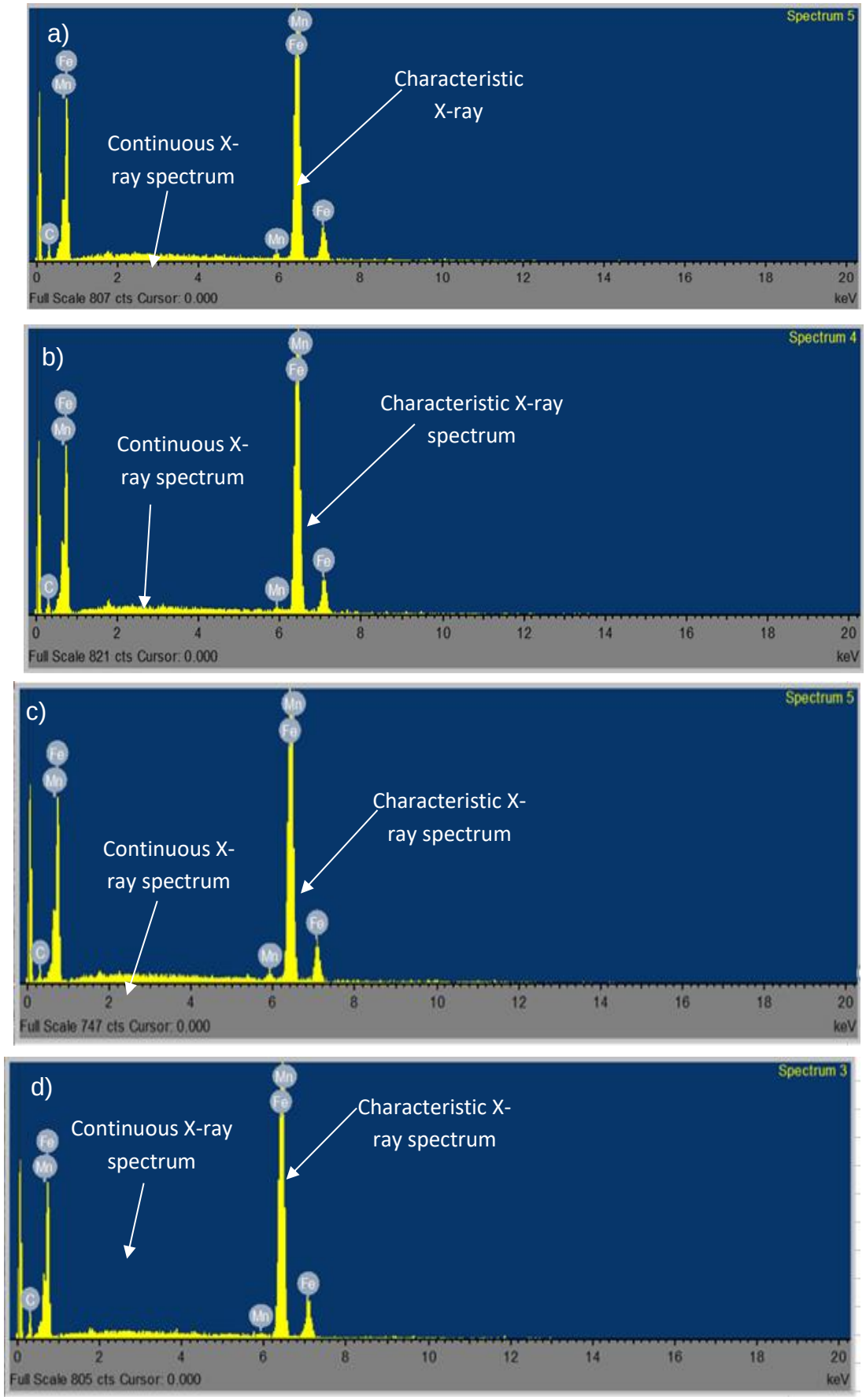

Figure 4.7: EDXS patterns of rail steel (a) base material – no fatigue load applied; (b) Specimen 1 – loaded for 6 min; (c) Specimen 2 – loaded for 8 min; (d) Specimen 3 – loaded for 10 min

4.3 Microhardness observation and analysis

This section discusses in-depth the microhardness results obtained. A hardness test was conducted across the entire length of specimens in three different lengths. The left-hand side highlighted on the mounted specimens (shown in Figure 4.8) is the head side, the surface where fatigue load was applied.

4.3.1 Microhardness test pattern

The four specimens tested in different intervals were carefully prepared for a Vickers microhardness test. The three lengths showing on tested specimens were described as upper, middle, and lower on each length. Indentations noticeable on specimens in Figure 4.8 (a) to (d) indicate this test pattern.

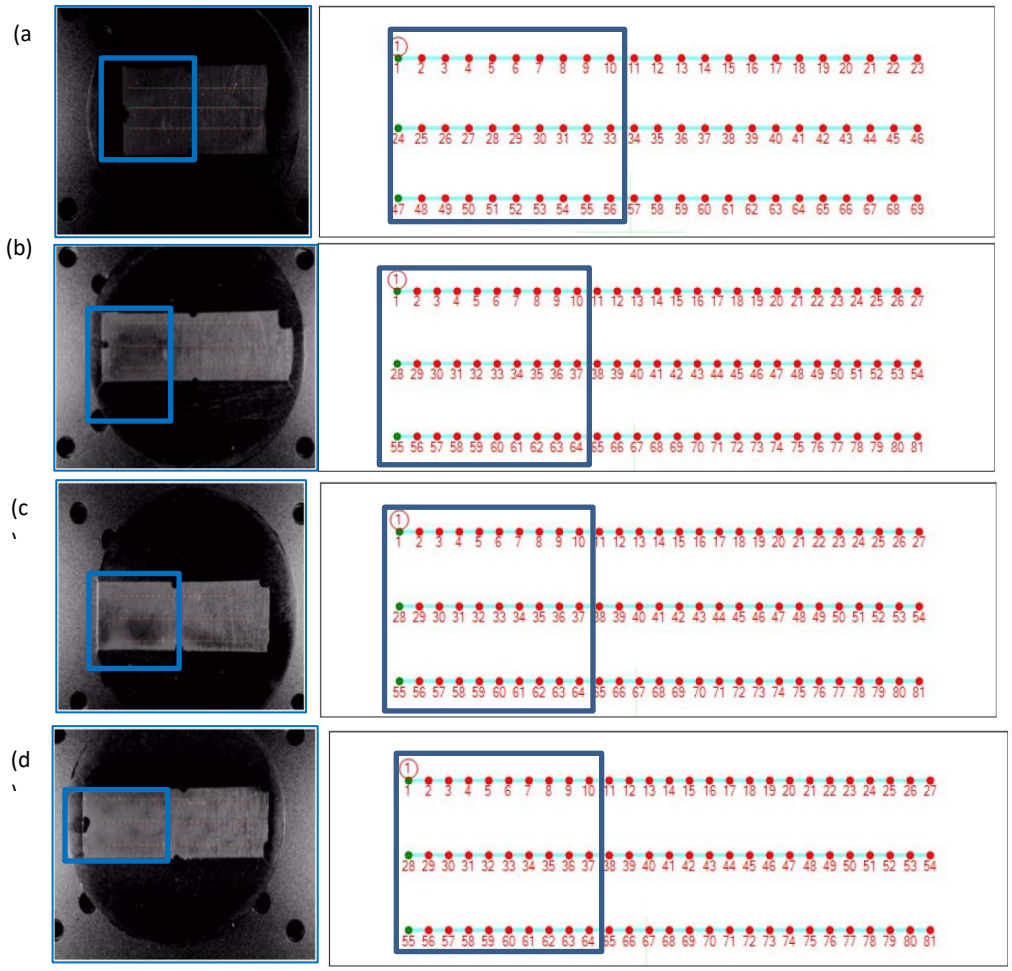

Figure 4.8: Specimens tested for microhardness showing test pattern (a) base material sample; (b) Specimen 1; (c) Specimen 2; (d) Specimen 3

4.3.2 Microhardness results

The graphs in Figure 4.9 and Table 4.5 illustrate the results of Vickers microhardness test performed on four samples; Table 4.5 presents the statistical analysis of the hardness values. The graph in Figure 4.9 (a), an observation of a base material sample, shows trends of lower hardness values with a maximum value of 389.53 HV0.5 (ref. Table 4.5). Figure 4.9 (d) shows the highest trend of hardness values, indicating an increase in hardness values. This is Specimen 3 which was placed under load for 10 minutes: its maximum value obtained is 443.34 HV0.5. The observed increase in hardness is caused by a repeated load applied for a longer period on the sample which resulted in the reduction of pearlite interlamellar spacing. It can be assumed that the rail line surface where the rail vehicle wheels contact the rail can develop plastic deformation due to drastic change in temperature caused by repetitive loading, weather conditions and frictional heat coming from the rolling contact load (Franklin *et al.*, 2008; Zhou *et al.*, 2020).

It is true that after many cycles of loading, the surface material hardens over time due to the high temperature on the contact surface and the development of a brittleness which renders the material more vulnerable to crack initiation and propagation. With the increase in rail hardness, the segment of broken cementite decreases, and the fraction of curled cementite increases These results correspond to the microstructure results observed with the Optical Microscope which have shown plastic deformation on Specimen 3 due to carbon content reduction (Masoumi *et al.*, 2019).

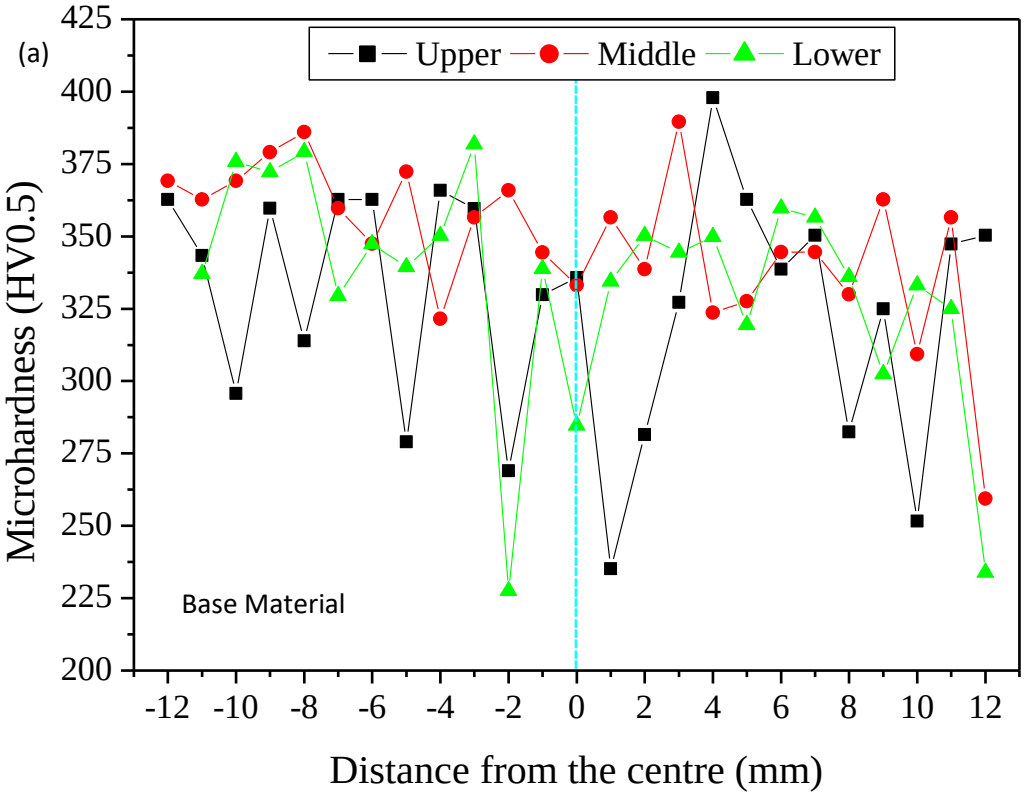
(a)
Upper
Middle
Lower
Microhardness (HV0.5)
Base Material
Distance from the centre (mm)

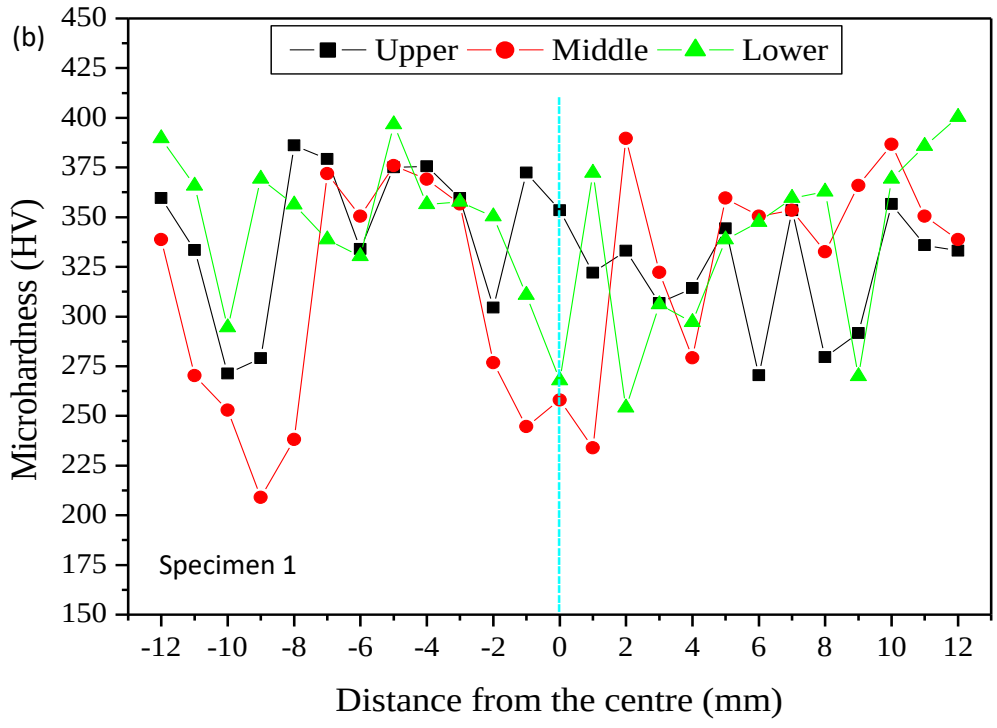
(b)
Upper
Middle
Lower
Microhardness (HV)
Specimen 1
Distance from the centre (mm)

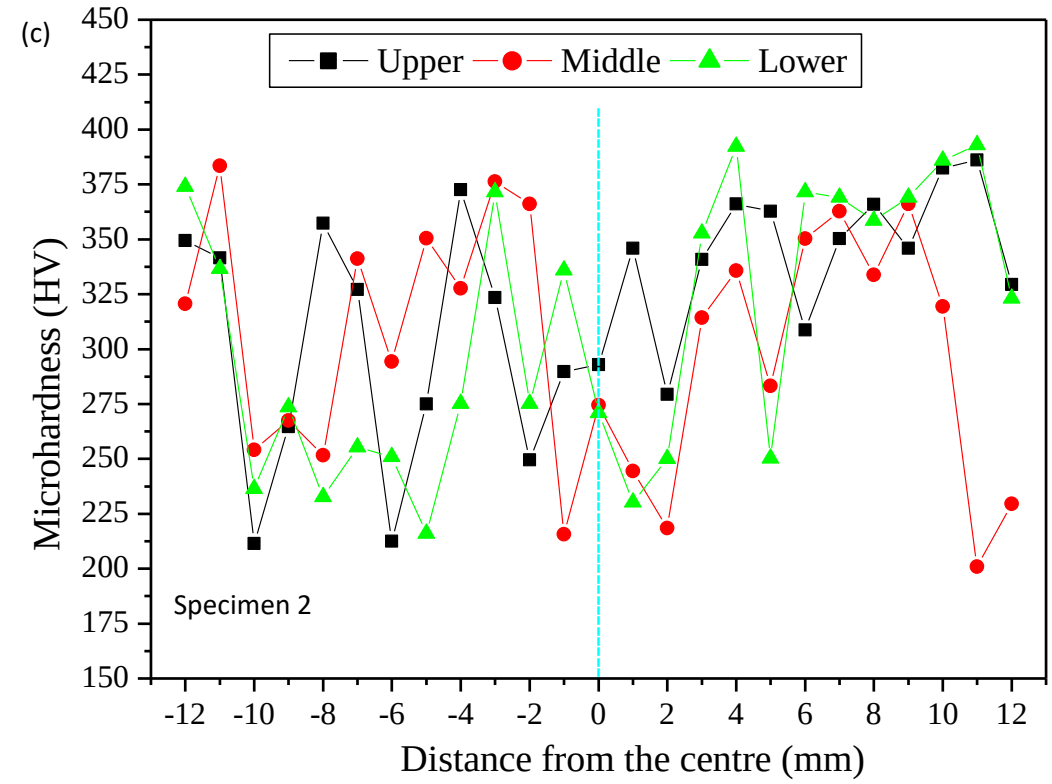

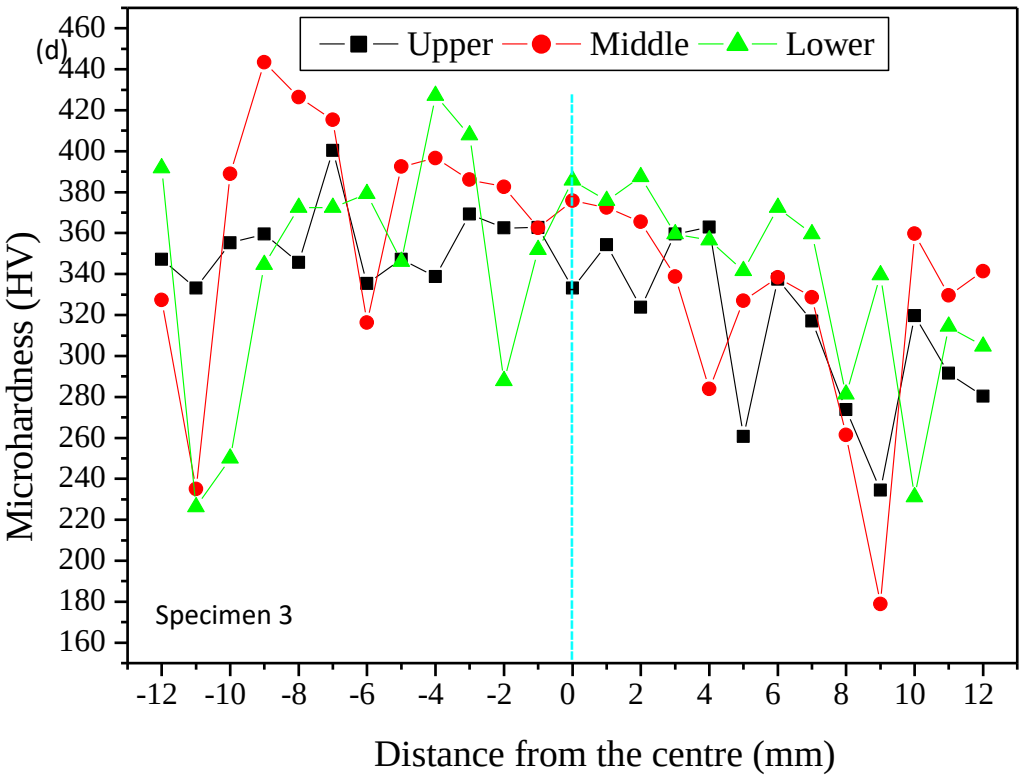

Figure 4.9: Microhardness profiles (a) base material; (b) Specimen 1; (c) Specimen 2; (d) Specimen 3

Table 4.5: Hardness statistical analysis: Vickers microhardness results (HV0.5)

Specimen	Mean	Min	Max	SD	Range
Base Metal	309.17	121.54	**389.5**	78	267.99
Specimen 1	270.03	101.34	**393**	79.8	289.11
Specimen 2	305.23	111.21	**400.3**	93.74	291.63
Specimen 3	311.79	123.75	**443.3**	89.2	319.59

CHAPTER 5

CONCLUSION AND RECOMMENDATIONS

5.1 Conclusion

The objective of this study was to analyse the impact of varying temperature conditions, together with fatigue, on the mechanical properties of the railway line. The virgin rail line steel was used in the study. The specimens were subjected to fatigue loading with one exception for the purpose of a benchmark comparison.

Microstructure and microhardness tests were conducted on the virgin rail material. Microstructural observations show the existence of ferrite grain boundaries and pearlite. The results show that rail steel microstructure transforms at the contact interface where repeated loading, which causes frictional heat, is occurring together with the environmental conditions. In this area, microstructural observations show the existence of ferrite at the grain boundaries and pearlite on the rail surface. Hardness test results reveal an increase in hardness values as the loading cycle time increases, while base material has lower hardness values. Higher hardness values on the loading surface indicate the development of a brittle material which is more vulnerable to crack initiation and propagation.

Specimens which were subjected to fatigue load have shown microstructure grain transformation and increased hardness when compared to the base metal. This clearly indicates that varying temperatures, together with fatigue, impact the mechanical properties of the railway line.

5.2 Recommendations

Railway lines need sufficient, regular care as railroad vehicles are in high demand in South Africa. Based on the results, there is a clear indication that temperature has an impact in the microstructure of the steel. If the material is left unattended, chances of developing defects are high. Rail line steel conditions change due to the transfer of rolling contact forces from the wheel of the rail vehicle to the rail line steel, and consequently this plays an important role in the material fatigue life. Therefore, regular inspection of rail lines is required to detect small deformations on the material and then to grind them to reduce defects from increasing. The process of a railway system is bound to experience too much stress due to rolling contact fatigue from multi-contacts of rail wheels, so manual inspection may not be adequate for detecting defects over time. Sensors would be the best solutions. The Railway Company should consider the installation of automated grease dispensing machines along the rails in areas where there is a high intensity of rail-wheel friction, such as on curves and where train speeds are at maximum.

More research is needed to elicit sufficient information about the maximum lifetime of the rail steel in busy areas so that the material can be replaced as soon as it has reached its maximum lifetime. This will assist in controlling rail steel microstructure and defects developing in the rail line.

To further understand grain transformation, it is recommended to compare a sample which has been in use but does not show any signs of defect with a virgin sample to see the actual appearance of the microstructure results of both.

LIST OF REFERENCES

1. Alonso, A. & Gime´nez, J.G. 2008. Wheel–rail contact: Roughness, heat generation and conforming contact influence. *Tribology International,* 41: 755-768.
2. Asih, A.M.S., and Kapoor, K.D.A. 2012). Modelling rail wear transition and mechanism due to frictional heating. *Wear*, 284-285: 82-90.
3. Athukorala, A.C., De Pellegrin, D.V., Kourousis, K. I. 2016. Characterization of head-hardened rail steel in terms of cyclic plasticity response and microstructure for improved material modelling. *Wear*, 366-367: 416-424.
4. Atroshenko, S.A., Mayer, S.S., and Smirnov, V.I. 2020. Analysis of the Fatigue Failure of Rail Steel. *Metals*, 62(10): 1573–1577.
5. Bansal, A.D., Ramachandran, N., and V Rastogi, V. 2019. Studies on the effects of braking loads on a Railway Wheel. *International Railway Journal*, 691.
6. Bhadeshia, H.K.D.H., Hasan, H.S. & Peet, M.J. 2011. Prediction of thermal conductivity of steel. *International Journal of Heat and Mass Transfer*, 54: 2602-2608.
7. Bird, J.O. & Ross, C. 2014*. Mechanical Engineering Principles*. New York: Routeledge.
8. Brehmer, M., Heyder, R., Mädler, K. & Zoll, A. 2008. Alternatives and Limits. *Rail Materials*, 1-9.
9. Carroll, R.I., and Beynon, J.H. 2006. Decarburization and rolling contact fatigue of a rail steel. *Wea*r, 260: 523-537.
10. Chapman, L., Thornes, J.E., Huang, Y., Cai, X., Sanderson, V.L. & White, S.P. 2008. Modelling of rail surface temperatures: a preliminary study. *Theoretical and Applied Climatology*. 92:121-131.
11. Chaves, A.P.G., Centeno, D.M.A., Masoumi, M., and Goldenstein, H. 2020. Effect of the Microstructure on the Wear Resistance of a Pearlitic Steel. *Materials Research*, 23(2): e20190605.

12. Chen, L., Yang, M., Yuacahao, X., Zhang, F., Zeyuan. & L Zhang, X. 2016. Effect of Cooling on Bonding Process of Heavy Rail after Rolling. *School of Material and Metallurgy, 3.*
13. Chen, R., Chen, J., Wang, P., Fang, J., and Xu, J. 2019. Impact of wheel profile evolution on dynamic interaction and surface initiated rolling contact fatigue in turnouts. *Wear*. 438–439.
14. Chen, Y., Ren, R., Zhao, X., Chen, C., and Pan, R. 2020. Study on the surface microstructure evolution and wear property of bainitic rail steel under dry sliding. *Wear*, 448-449.
15. Chinowsky, P., Helman, J., Gulati, S., Neumann, J., and Martinich, J. 2019. Impacts of climate change on operation of the US rail network. *Transport Policy*, 75: 183-191.
16. Cvetkovski, K., and Ahlstrom, J. 2013. Characterization of plastic deformation and thermal softening of the surface layer of railway passenger wheel treads. *Wear*, 300(1-2): 200-204.
17. Demir, A. & Fazil, O. 2007. Analytical relations between hardness and strain for the cold formed parts. *Journal of Materials Processing Technology,* 186: 163-173.
18. Dobney K., Baker C.J., Chapman L. and Quinn A.D. 2010. The future cost to the United Kingdom's railway network of heat-related delays and buckles caused by the predicted increase in high summer temperatures owing to climate change. *Scopus,* 224(1):25 – 341
19. Duan, Z., Liu, Y., Wang, L., Wei, Y. & Wu, Y. 2017. 3-D analysis of thermal-mechanical behavior of rail-wheel sliding contact considering temperature characteristics of materials. *Applied Thermal Engineering*, 115: 455–462.
20. Edel, K.O., Lundén, R., Smith, R. A. & Zerbst, U. 2009. Introduction to the damage tolerance behaviour of railway rails - a review. *Engineering Fracture Mechanics,* 76:2563–2601
21. Ekberg, A., and Pålsson, B.A. 2019. Multiscale modelling of train–track interaction phenomena with focus on contact mechanics, *Wear*, 430–431: 393-400.

22. Fang, X.Y., Zhaoa, Y.X. and Liu, H. 2017. Study on fatigue failure mechanism at various temperatures of a high-speed railway wheel steel. *Materials Science & Engineering*, 696: 299 –314.
23. Ferranti, E., Chapman, L., Lowe, C., McCulloch, S., Jaroszweski, D., Quinn, A. 2016. Heat-related failures on southeast England's railway network: Insights and implications for heat risk management. *Weather, Climate, and Society, p*p 177–191
24. Franklin, F.J., Garnham, J.E., Fletcher, D.I., Davis, C.L. and Kapoor, A. 2008. Modelling rail steel microstructure and its effect on crack initiation. *Wear*, 265: 1332–1341
25. Garcia-Sanchez, D., Sanudo, R., Miranda, M., Tarrago, N., and Lenart, S. 2021. Rail expansion devices and maximum dilation length in railway bridges. An experimental study. *Engineering Structures*, 229.
26. Godefroid, L. G., Souza, A.T., Maria, A. 2020. Fracture toughness, fatigue crack resistance and wear resistance of two railroad steels. *Journal of Materials Research and Technology*, 9(5):9588-9597.
27. Hong, S., Kim, H (Uk)., Lim, N.H., Kim, K.H., Kim, H. and Cho, S.J. 2019. A Rail-Temperature-Prediction Model Considering Meteorological Conditions and the Position of the Sun. *International Journal of Precision Engineering and Manufacturing*. 20:337–346.
28. Hu, Y., Watson, M., Maiorino, M., Zhou, L., Wang, W.J., Ding, H.H., Lewis, R., Meli, E., Rindi, A., Liu, Q.Y., and Guo, J. 2021. Experimental study on wear properties of wheel and rail materials with different hardness values. *Wear*, 477:203831
29. Hu, Y., Zhou, L., Ding, H.H., Tan, G.X., Lewis, R., Liu, Q.Y., Guo, J., and Wang, J.W. 2020. Investigation on wear and rolling contact fatigue of rail-wheel materials under various rail-wheel hardness ratio and creepage conditions. *Tribology Research Institute*, 143:106091
30. Ishida, M. 2013. Rolling contact fatigue (RCF) defects of rails in Japanese railways and its mitigation strategies. *Electronic Journal of Structural Engineering*, 13(1):67-74.

31. Jun, H.K., Seo, J.W., Jeon, I.S., Lee, S.H. and Chang, Y.S. 2016. Fracture and fatigue crack growth analyses on a weld-repaired railway rail. Engineering Failure Analysis, 59:478-492.
32. Kang, C., Schneider, S., Wenner, M., and Marx, S. 2021. Experimental investigation on the fatigue behavior of rails in the transverse direction. *Construction and Building Materials*, 272:121666.
33. Koetse M.J. & Rietveld, P. 2009. The impact of climate change and weather on transport: An overview of empirical findings. *Transportation Research Part D*, 14:205-221.
34. Lewis, R., Christoforou, P., Wang, W.J., Beagles, A., Burstow, M., and Lewis, S.R. 2019 Investigation of the influence of rail hardness on the wear of rail and wheel materials under dry conditions. *Wear*, 430-431.
35. Lewis, R., and Olofsson, U. (eds). 2009. *Technology & Engineering: Rail-wheel Interface Handbok*. Boston: Woodhead.
36. Li, Y., Zhang, F., Chen, C., Lv, B., Yang, Z., and Zheng, C. 2016. Effects of deformation on the microstructures and mechanical properties of carbide–free bainitic steel for railway crossing and its hydrogen embrittlement characteristics. *Materials Science & Engineering: A*, 651: 945-950.
37. Liu, X., Xiao, C., and Meehan, P.A. 2019. The effect of rolling speed on lateral adhesion at rail-wheel interface under dry and wet condition. *Wear*, 438-439:203073 .
38. Long, X.Y., Branco, R., Zhang, F.C., Berto, F., and Martins, R.F. 2020. Influence of Mn addition on cyclic deformation behaviour of bainitic rail Steels. *International Journal of Fatigue*, 132: 105362
39. Ma, L., Shi, L.B., Guo, J., Liu, Q.Y. and Wang, W.J. 2018. On the wear and damage characteristics of rail material under low temperature environment condition. *Wear*. 394-395:149 -158
40. Ma, L., Guo, J., Liu, Q.Y. and Wang, W.J. 2017. Fatigue crack growth and damage characteristics of high-speed rail at low ambient temperature. *Engineering Failure Analysis.* 82:802-815
41. Masoumi, M., Ariza, E.A., Sinatora, A. and Goldenstein, H. 2018. Role of crystallographic orientation and grain boundaries in fatigue crack

propagation in used pearlitic rail steel. *Materials Science & Engineering A*, 722:147-155

42. Masoumi, M., Echeverri, E.A.A, Tschiptschin, A.P. and Goldenstein, H 2019, Improvement of wear resistance in a pearlitic rail steel via quenching and partitioning processing. Scientific Reports, 9:7454.
43. Masoumi, M., Sinatora, A. and Goldenstein, H. 2019 'Role of microstructure and crystallographic orientation in fatigue crack failure analysis of a heavy haul railway rail. *Engineering Failure Analysis,* 96:320-329
44. Matsumura, O., Y. Sakuma, Y. & Takechi, H. 1991. Mechanical properties and retained austenite in intercritically heat-treated bainite-transformed steel and their variation with Si and Mn additions. *Metallurgical Transactions A: Mechanical Behaviour,* 22(2):489-498.
45. Meyer, K. A., Nikas, N., and Ahlström, J. 2018. Microstructure and mechanical properties of the running band in a pearlitic rail steel: Comparison between biaxially deformed steel and field samples. *Wear.* 396-397:12-21
46. Mirkovic, N., Brajovic, L., Popovic, Z., Todorovic, G., Lazarevic, L., Petrovic, M. 2021. Determination of temperature stresses in CWR based on measured rail surface temperatures. *Construction and Building Materials*, 284
47. Mishra, K., and Singh, A. 2017. Effect of interlamellar spacing on fracture toughness of nano-structured pearlite. *Materials Science and Engineering: A*, 706: 22-26.
48. Mitao, S., Takemasa, M and Yokoyama, H. 2002. Development of High Strength Pearlitic Steel Rail (SP Rail) with Excellent Wear and Damage Resistance. *NKK Technical Review,* 86:1-7.
49. Molyneux-Berry, P., Davis, C., and Bevan, A 2014. The Influence of Rail-wheel Contact Conditions on the Microstructure and Hardness of Railway Wheels. *The Scientific World Journal*, 214: 209752
50. Msomi, V., Basson, C.C. P., and Mabuwa, S. 2020. Microstructural analysis of rail tracks defects: case study. *Materials Science and Engineering,* 892: 012002.

51. Nejad, R.M. 2020. Numerical study on rolling contact fatigue in rail steel under the influence of periodic overload. *Engineering Failure Analysis*, 115: 104624.
52. Outinen, J. & Makelainen, P. 2004. Mechanical properties of structural steel at elevated temperatures and after cooling down. *Fire and Material. 28(2-4):237 – 251.*
53. Poya, N. (CEO of Railway Safety Regulator. 2015. State of Safety Report 2013/ 2014: Operational occurrences and security-related incidents. South Africa. Government. Public Service. Centurion.
54. Pyke, D. 2020. Daniel Pyke's profile page [LinkedIn]. [Accessed 29 May 2021]. https://www.linkedin.com/pulse/rail-101-why-rails-fail-more-often-winter-daniel-pyke/
55. Qiu, J., Zhang, M., Tan, Z., Gao, G., and Bai, B. 2019. Research on the Microstructures and Mechanical Properties of Bainite/Martensite Rail Treated by the Controlled-Cooling Process. *Materials (Basel)*, 12(19):3061.
56. Railway Safety Regulator State of Safety Report 2019/20 State of Safety Report 2019/2020: Operational occurrences and security-related incidents. South Africa, Government. Public Service. Centurion.
57. Razhkovskiy, A.A., Bunkova, T.G., Petrakova, A.G., and Omsk, O.V.G. 2015 Optimization of Hardness Ratio in Rail–Wheel Friction Pair. *Journal of Friction and Wear*, 36(4): 433–442.
58. Rossetti, M.A., 2002. Potential impacts of climate change on railroads. *The Potential Impacts of Climate Change on Transportation Workshop, USDOT Centre for Climate Change and Environmental Forecasting.*
59. Sanchisa, I.V., Francoa, R.I., Zuriaga, P.S & Fernándeza, P.M. 2020. Risk of increasing temperature due to climate change on high-speed rail network in Spain. *Transportation Research Procedia.* 45:5–12.
60. Shi, L.B., Ma, L., Guo, J., Liu, Q.Y., Zhou, Z.R. and Wang, W.J. 2018. Influence of low temperature environment on the adhesion characteristics of contact. Tribology International. 127:59-68.
61. Sundh, J. and Olofsson, U. 2011. Relating contact temperature and wear transitions in a wheel–rail contact. Wear. 271 (1-2):78–85.

62. Thaduri, A., Galar, D., and Kumar, U. 2020. Space weather climate impacts on railway infrastructure. *Int J Syst Assur Eng Manag*. 11: 267–281.
63. Ueda, M., and Matsuda, M. 2020. Effects of carbon content and hardness on rolling contact fatigue resistance in heavily loaded pearlitic rail steels. *Wear*, 444-445: 203120.
64. Vo, K.D., Tieu, A.K., Zhu, H. T. and Kosasih, P.B 2015. The influence of high temperature due to high adhesion condition on rail damage. *Wear,* 330–331: 571-580.
65. Walters, C.L. 2014. The effect of low temperatures on the fatigue of high-strength structural grade steels. *Procedia Material Science, 3*: 09 – 214.
66. Walters, C.J., Alvaro, J. and Maljaars, J. 2016. The effect of low temperatures on the fatigue crack growth of S460 structural steel. *International Journal of Fatigue*. Part 1, 82: 110-118.
67. Wang, C., Shi, L.B., Ding, H.H., Wang, W.J., R. Galas, R., Guo, J., Liu, Q.Y., Zhou, Z.R., and Omasta, M. 2021, Adhesion and damage characteristics of rail-wheel using different mineral particles as adhesion enhancers. *Wear*. 477, 18: 203796
68. Wang, G., Qu, S., Lianmin, Y., Li, X., Yue, W., Fu, Z. & Farhangdoost, K. 2016. Rolling contact fatigue property and failure mechanism of carburized 30CrSiMoVM steel at elevated temperature. Tribology International. 98:144-154.
69. Wang, W.J., Shen, P., Song, J.H. Guo, J., Liu, Q.Y., and Jin, X.S. 2011. Experimental study on adhesion behavior of rail-wheel under dry and water conditions. *Tribology Research Institute*, 279(9-10): 2699-2705.
70. Wang, W.J., Lewis, R., Yang, B., Guo, L.C., Liu, Q.Y. and Zhu, M.H. 2016. Wear and damage transitions of wheel and rail materials under various contact conditions. *Wear.* 362–363:146 – 1562.
71. Wang, Y., XI, W. and Shi, Y. 2007. Experimental study of the impact toughness of rail steel at low temperatures. *Research Gate.*
72. Wen, J., Marteau, J., Bouvier, S., Risbet, M., Cristofari, F., and Secordel, P. 2020. Comparison of microstructure changes induced in two pearlitic

rail steels subjected to a full-scale rail-wheel contact rig test. Technological Research Institute, 456-45: 203354.

73. Xu, W., Zhang, B., Deng, Y., Wang, Z., Jiang, Q., Yang, L. and Zhang, J. 2021. Corrosion of rail tracks and their protection. *Review*. 39(1): 1–13.
74. Zhang, F., Yang, Y., Shan, Q., Li, Z., Bi, J. and Zhou, R. 2020. Microstructure Evolution and Mechanical Properties of 0.4C-Si-Mn-Cr Steel during High Temperature Deformation. Materials (Basel), 13(1): 172.
75. Zhou, L., Hu, Y., Ding., H.H., Liu, Q.Y., Guo, J., and Wang, W.J. 2021. Experimental study on the wear and damage of rail-wheel steels under alternating temperature conditions. *Wear,* 477: 203829
76. Zhou, L., Wang, WJ., Hu, Y., Marconi, S., Meli, E., Ding, H.H., Liu, Q.L., Guo, J., and Rindi, A. 2020. Study on the wear and damage behaviours of hypereutectoid rail steel in low temperature environment. *Wear.* 456–457: 203365.